J-910904-1

Analytical Study of the Spectral Radiant Flux Emitted from the Fuel Region of a Nuclear Light Bulb Engine

Contract No. SNPC-70

UNITED AIRCRAFT CORPORATION

United Aircraft Research Laboratories

EAST HARTFORD, CONNECTICUT

United Aircraft Research Laboratories

UNITED AIRCRAFT CORPORATION

EAST HARTFORD, CONNECTICUT

J-910904-1

Analytical Study of the Spectral Radiant Flux Emitted from the Fuel Region of a Nuclear Light Bulb Engine

Contract No. SNPC-70

REPORTED BY N. L. Krascella

APPROVED BY W. G. Burwell
W. G. Burwell, Chief
Kinetics and Thermal
Sciences

DATE September 1970

NO. OF PAGES 52

COPY NO. 26

FOREWORD

An exploratory experimental and theoretical investigation of gaseous nuclear rocket technology is being conducted by the United Aircraft Research Laboratories under Contract SNPC-70 with the joint AEC-NASA Space Nuclear Propulsion Office. The Technical Supervisor of the Contract for NASA is Captain C. E. Franklin (USAF). Results of portions of the investigation conducted during the period between September 16, 1969 and September 15, 1970 are described in the following eight reports (including the present report) which comprise the required first Interim Summary Technical Report under the Contract:

1. Klein, J. F. and W. C. Roman: Results of Experiments to Simulate Radiant Heating of Propellant in a Nuclear Light Bulb Engine Using a D-C Arc Radiant Energy Source. United Aircraft Research Laboratories Report J-910900-1, September 1970.

2. Jaminet, J. F. and A. E. Mensing: Experimental Investigation of Simulated-Fuel Containment in R-F Heated and Unheated Two-Component Vortexes. United Aircraft Research Laboratories Report J-910900-2, September 1970.

3. Vogt, P. G.: Development and Tests of Small Fused Silica Models of Transparent Walls for the Nuclear Light Bulb Engine. United Aircraft Research Laboratories Report J-910900-3, September 1970.

4. Roman, W. C.: Experimental Investigation of a High-Intensity R-F Radiant Energy Source to Simulate the Thermal Environment in a Nuclear Light Bulb Engine. United Aircraft Research Laboratories Report J-910900-4, September 1970.

5. Bauer, H. E., R. J. Rodgers and T. S. Latham: Analytical Studies of Start-Up and Dynamic Response Characteristics of the Nuclear Light Bulb Engine. United Aircraft Research Laboratories Report J-910900-5, September 1970.

6. Latham, T. S. and H. E. Bauer: Analytical Studies of In-Reactor Tests of a Nuclear Light Bulb Unit Cell. United Aircraft Research Laboratories Report J-910900-6, September 1970.

7. Palma, G. E. and R. M. Gagosz: Optical Absorption in Transparent Materials During 1.5 Mev Electron Irradiation. United Aircraft Research Laboratories Report J-990929-1, September 1970.

8. Krascella, N. L.: Analytical Study of the Spectral Radiant Flux Emitted from the Fuel Region of a Nuclear Light Bulb Engine. United Aircraft Research Laboratories Report J-910904-1, September 1970. (present report)

Report J-910904-1

Analytical Study of the Spectral Radiant Flux Emitted from the Fuel Region of a Nuclear Light Bulb Engine

TABLE OF CONTENTS

TABLE OF CONTENTS
(Cont'd.)

Report J-910904-1

Analytical Study of the Spectral Radiant Flux Emitted from the Fuel Region of a Nuclear Light Bulb Engine

SUMMARY

A theoretical investigation was conducted to determine the spectral distribution of radiative flux emitted from the fuel region of a nuclear light bulb engine and, hence, the spectral radiative flux incident upon the transparent containment walls or upon the reflective end walls of such an engine. The analysis was performed for a specified engine configuration, for a specified nuclear fuel partial pressure distribution and for a total of 47 wave numbers. A total of six cases were calculated to investigate the effect on the spectral radiative flux of changes in total radiated flux, seed gas partial pressure, and end-wall reflectivity. The total radiated flux was changed from a reference value of 24,300 to 48,600 Btu/ft^2-sec. The effect of seed gases was examined by the addition of a mixture of 5 atm each of oxygen and nitric oxide. Wall reflectivity was examined by employing the spectral reflectivity of aluminum and silver in place of a zero-reflectivity wall employed in the reference case.

CONCLUSIONS

1. The spectral distribution of radiative flux emitted from the nuclear fuel region of a nuclear light bulb engine differs appreciably from that of a black body at the assumed radiating temperature of 15,000 R. Increasing the effective black-body radiating temperature from 15,000 to 17,838 R (equivalent to doubling the total radiated flux) increases the spectral flux at all wave numbers but does not appreciably alter the spectral distribution of radiated energy.

2. For a nuclear fuel system emitting energy at an effective black-body radiating temperature of 15,000 R, the addition of a seed mixture of 5 atm of oxygen and 5 atm of nitric oxide attenuates the radiation emitted radially in the ultraviolet region of the spectrum to a level less than that of a 15,000 R black-body.

3. Use of reflective end walls tends to shift the spectral distribution of energy radiated axially toward the ultraviolet spectral region (toward higher wave numbers). The ultraviolet shift in the spectral distribution is greater for aluminum reflective end walls than for silver reflective end walls.

4. Seeding with an oxygen-nitric oxide seed mixture in a fuel region bounded by reflective end walls reduces the fraction of radiation emitted axially in the ultraviolet spectral region. The reduction in this case is considerably less than the corresponding reduction in the ultraviolet radiation emitted in a radial direction.

INTRODUCTION

Analytical and experimental investigations of various aspects of gaseous nuclear rocket technology are currently being conducted by the Research Laboratories of United Aircraft Corporation under Contract SNPC-70 administered by the joint AEC-NASA Space Nuclear Propulsion Office. Of primary interest under this contract is the nuclear light bulb engine concept described in Ref. 1. In this concept, a vortex-stabilized gaseous nuclear reactor emits thermal radiation which is utilized to heat a seeded hydrogen propellant. The nuclear fuel and seeded propellant regions are physically separated by an internally cooled transparent wall. Knowledge of the spectral distribution of thermal radiation emitted from the nuclear fuel region and subsequently incident upon the transparent containment wall or reflective end wall is necessary in analyzing the feasibility of the nuclear light bulb engine concept.

Previous calculations performed at UARL indicated that the spectral distribution of radiative energy emitted from the nuclear fuel region differs appreciably from that of a black body at an effective radiating temperature of 15,000 R (Ref. 2). These studies revealed that approximately 17 percent of the total radiated flux (24,300 Btu/ft^2-sec) is emitted at wave numbers greater than about 55,000 cm^{-1} where the transparent containment wall becomes essentially opaque. Thus, the need for effective seeding of the fuel to prevent ultraviolet radiation from impinging upon the transparent containment walls was demonstrated. Preliminary calculations were made to evaluate the effectiveness of hydrogen as a seed gas. Although hydrogen would effectively block radiation emitted from the fuel region at wave numbers greater than 105,000 cm^{-1}, hydrogen is essentially transparent in the wave number range between 55,000 and 105,000 cm^{-1}. It became necessary then to evaluate the effectiveness of other candidate seeding materials.

An additional problem is encountered when considering radiation emitted from the fuel region in an axial direction. Axially directed radiation impinges upon highly reflecting end walls in the full-scale engine; a substantial fraction of the incident radiation is expected to be reflected. Previous studies with a hypothetical uniformly reflecting end wall and an aluminum end wall indicated a marked increase in the axial edge-of-fuel temperature as well as a shift in the axial spectral flux distribution toward the ultraviolet region of the spectrum (Ref. 2). No comparisons were made between the effects of aluminum and other possible metallic reflecting end-wall materials. Similarly, the use of seed gases in the axial cases has not been considered.

Based on the preceding discussion, a program was formulated to determine the effects on the temperature distributions within and the spectral distributions of

radiation emitted from the fuel region of a nuclear light bulb engine of: (a) adding an effective seed gas, (b) increasing the total radiative flux (corresponding to an increase in effective black-body radiating temperature) and (c) including different reflective end-wall materials. The program is described in detail in succeeding sections of this report.

ANALYTICAL METHOD

The radiation spectrum emitted from the fuel region of a nuclear light bulb engine is determined by conditions in the outermost layer of the region due to the high opacity of the nuclear fuel. At the temperatures and pressure anticipated in the full-scale device, the dominating layer is typically a few centimeters in depth; therefore the region may be considered as a plane-parallel gas layer containing a relatively low concentration of nuclear fuel. Since low nuclear fuel density in the edge-of-fuel region precludes extensive energy generation by nuclear fission in this region, the outermost layer of fuel is characterized by a constant total energy flux at all positions within the region.

The spectral distribution of flux emitted from the fuel-containment region may be estimated using a transport analysis of the radiative transfer process. The radiation flux profile is a function of the temperature distribution in the outer fuel layer as well as the composition and spectral absorption coefficients of the nuclear fuel. These fuel properties are functions of both pressure and temperature.

Iterative Procedure

The temperature and corresponding spectral radiative flux profiles in the edge-of-fuel region may be determined for a specified fuel partial pressure distribution by means of an iterative procedure utilizing existing one-dimensional UARL simplified grey-gas and spectral transport computer codes. The iterative procedure is briefly outlined in the following paragraph. A more detailed description is presented in Ref. 2.

Initially, the simplified grey-gas computer code is used to define a temperature profile in the edge-of-fuel region using the optically thick approximation. The temperature profile is determined for a specified fuel partial pressure distribution, an assumed Rosseland mean opacity distribution, a specified edge-of-fuel temperature and a uniform specified total flux, Q^*. The estimated temperature profile and fuel partial pressure distribution are used in the spectral transport computer code to calculate the spectral flux distribution, Q_ω at various positions within the outer layer of fuel. The calculated spectral fluxes at each position are integrated to ascertain the total flux, Q_T. Convergence is confirmed if the calculated total flux, Q_T, and the specified total flux Q^* are within five percent at all positions within the fuel region. In addition, the uniform flux condition requires that the net energy deposited at any position must be essentially zero to confirm convergence. The procedure is repeated modifying the assumed Rosseland mean opacity distribution and/or the edge-of-fuel temperature until the requirements for convergence are fulfilled. Generally, 10 to 15 iterations are required to achieve convergence.

Unit Cavity Configuration and Pressure Distribution

A fuel containment region 0.681 ft (20.75 cm) in depth at a total pressure of 500 atm was selected for the spectral radiation emission analysis of the nuclear light bulb engine unit cavity schematically depicted in Fig. 1. It was assumed that nuclear fuel existed at a constant pressure of 200 atm from the centerline of the containment region out to a depth of 0.3405 ft (10.38 cm). At positions between 0.3405 ft and the edge of fuel the fuel partial pressure decreased linearly with distance as shown in Fig. 2. Since the calculational procedure in the spectral transport code requires a positive pressure of absorbing material at all positions for which estimates of radiation transfer are made, studies involving pure fuel (no seeds - cases 1, 2, 4 and 5) assumed an edge-of-fuel partial pressure of 0.01 atm while studies involving seed gases (positive seed gas partial pressure at the edge-of-fuel - cases 3 and 6) assumed no fuel at the edge-of-fuel position. The difference between the total pressure of 500 atm and the fuel partial pressure at any position was attributed to neon (the absorption due to neon was neglected). Note that distances, y, in the fuel region are measured from the edge of fuel (y = 0) inward toward the centerline (y = 20.75 cm). For cases 1, 2 and 3 (without reflective walls) the distance, y, is measured radially: for cases 4, 5 and 6 (with reflective end walls) the distance, y, is measured axially (see Fig. 1).

Description of Gases

The iterative procedure, cavity configuration and partial pressure distributions described in preceding paragraphs were employed in all subsequent calculations of the radiative spectral flux distributions emanating from the nuclear fuel containment region of a nuclear light bulb engine. Six cases were treated in which the effect of (1) doubling the total radiated flux, (2) the addition of an oxygen-nitric oxide seed mixture, (3) inclusion of different reflective end-wall materials and (4) the addition of the seed gas mixture in combination with a reflective end wall on the spectral distribution of energy radiated from the nuclear fuel region were studied.

The heavy-atom model (Refs. 2, 3 and 4) used to calculate the requisite fuel composition and spectral absorption characteristics as a function of temperature and pressure for use as input in the spectral transport computer code was the same for cases 1 through 6. The fuel species ionization potentials were 6.1, 11.46, 17.94 and 31.14 ev (Ref. 5). In addition, a band type oscillator strength distribution function required by the heavy-atom model and described in Ref. 6 was used for all cases examined. All spectral quantities were calculated for forty-seven wave numbers as compared to approximately twenty-five wave numbers for previous studies reported in Ref. 2. The increase in the number of spectral determinations was made in order to obtain more detailed spectral information at wave numbers greater than approximately 55,000 cm^{-1} where the transparent wall material begins to lose transparency.

In cases 1 and 2, the effect of doubling the total radiative flux from 24,300 to 48,600 Btu/ft^2-sec(corresponding to a change in effective black-body radiating temperature from 15,000 to 17,838 R) on the spectral distributions of flux emitted radially from the fuel region was studied. Calculations for cases 1 and 2 involved only pure fuel; no seed gases were considered.

The effect of the addition of a uniform partial pressure of 5 atm of oxygen (O_2) and 5 atm of nitric oxide (NO) as a seed gas mixture on the radially emitted spectral flux distribution was determined in case 3 for a total radiative flux of 24,300 Btu/ft^2-sec.

Cases 4 and 5 represent a comparison of end-wall effects in which a fraction of the axially emitted flux from the fuel region is reflected back into the fuel region by end walls of aluminum (case 4) and silver (case 5) for a total radiative flux of 24,300 Btu/ft^2-sec. Spectral reflectivities for aluminum (Refs. 7 through 10) and silver (Refs. 11 and 12) are graphically depicted in Fig. 3. Seed gases were not considered in these cases.

In case 6, the combined effect of reflective end walls and an oxygen-nitric oxide seed gas mixture on the axially emitted spectral flux distribution was studied for a total radiative flux of 24,300 Btu/ft^2-sec. Calculations were made for a fuel region bounded by aluminum end walls and containing a uniform distribution of five atm each of oxygen and nitric oxide.

The various conditions and approximations as well as a summary of various figures are compiled in Table I for reference.

SPECTRAL DISTRIBUTION OF RADIANT ENERGY FROM THE NUCLEAR FUEL REGION

Temperature Distributions

Ten to fifteen iterations were required in each case to achieve convergence between the simplified grey-gas code and the spectral transport code. As noted previously, convergence was based on the criteria of essentially uniform total flux and the associated negligible energy loss at all axial or radial positions for which the calculations were made. Edge-of-fuel temperatures as estimated by the iterative procedure for cases 1 through 6 are as follows: case 1, 10,650 R; case 2, 12,650 R; case 3, 11,650 R; case 4, 23,650 R; case 5, 17,650 R; case 6, 24,650 R. Temperature distributions in the outermost layer of the fuel containment region are compared for all six cases in Fig. 4 as a function of distance, y, measured from the edge of fuel.

Comparison of the results for cases 1, 2 and 3 plotted in Fig. 4 show the effect of doubling the total radiated flux (case 2) and addition of an oxygen-nitric oxide seed gas (case 3) on the temperature distributions in the outer layer of the fuel containment region. In general, doubling the total radiated flux increases the temperature at any position in the fuel region by approximately 2,200 R; addition of the seed gas results in a temperature distribution which is approximately 1,100 R greater than the pure fuel case. No appreciable difference in temperature gradients at any position in the fuel region is evident in the results shown for cases 1, 2 and 3.

The curves for case 4 (aluminum end walls) and case 5 (silver end walls) exhibit the effect of different end-wall reflectivities on axial temperature distributions. Marked increases in temperature at any position in the fuel region are noted for the reflective end wall cases as compared to case 1. Similarly, the results graphically depicted in Fig. 4 for case 6 show the anticipated increase in the axial temperature distribution as a result of including an oxygen-nitric oxide seed mixture with reflective end walls of aluminum.

Spectral Absorption Coefficients

Typical spectral absorption coefficient results calculated by means of the spectral transport code at the edge-of-fuel temperatures are compared in Fig. 5 for cases 1 and 2, in Fig. 6 for cases 1 and 3, in Fig. 7 for cases 1, 4 and 5 and in Fig. 8 for cases 1, 4 and 6. These data and similar data at other axial or radial positions, representing different conditions of temperature and pressure, are required for the spectral analysis of radiation emitted from the fuel-containment region. Such data near the edge of fuel are particularly significant, since the absorption coefficients of the peripheral gas layer are most influential in determining the spectral emission characteristics of the fuel-containment region.

Qualitatively, a strong peak in spectral absorption coefficient of the material near the edge of fuel will cause a valley in the spectral distribution results for the emitted radiation. Conversely, a marked valley in the spectral absorption coefficient of the material near the edge of fuel will cause a strong peak in the spectral distribution results for the emitted radiation.

The spectral absorption coefficients of the nuclear fuel at a partial pressure of 0.01 atm are illustrated in Fig. 5 for a temperature of 10,650 R, the edge-of-fuel temperature for case 1, and for a temperature of 12,650 R, the edge-of-fuel temperature for case 2.

In Fig. 6 a comparison is made of the spectral absorption coefficient of 0.01 atm of pure fuel at a temperature of 10,650 R (edge-of-fuel temperature for case 1) and the spectral absorption coefficient of a mixture of 5 atm of oxygen and 5 atm of nitric oxide at the edge-of-fuel temperature for case 3 of 11,650 R.

Spectral absorption coefficient results for pure fuel at a partial pressure of 0.01 atm are compared in Fig. 7 for case 1 with a temperature of 10,650 R, case 4 with a temperature of 24,650 R and for case 5 with a temperature of 17,650 R. Case 4 involves reflective end walls of aluminum and case 5 involves reflective end walls of silver. Since seed gases are not considered in cases 1, 4 and 5, the results shown in Fig. 7 exhibit the change in the spectral absorption coefficient of nuclear fuel with temperature.

Similar comparisons of the spectral absorption coefficient distributions of 5 atm of oxygen and 5 atm of nitric oxide at a temperature of 24,650 R (case 6) and nuclear fuel at a partial pressure of 0.01 atm and at temperatures of 10,650 R (case 1) and 23,650 R (case 4) are presented in Fig. 8. Case 1, used as a standard of comparison, considered pure fuel with no reflective end walls; in case 4, an end wall of aluminum was considered; in case 6, an oxygen-nitric oxide seed mixture as well as reflective end walls of aluminum were treated.

In addition to the results presented for specific cases studied, a comparison of the spectral absorption properties of the seed mixture (5 atm of oxygen and 5 atm of nitric oxide) at various temperatures is shown in Fig. 9. These results were computed from spectral absorption cross-section data from Refs. 13, 14 and 15 and composition data for the oxygen-nitric oxide mixture which were computed at UARL. The composition calculations indicated that the principal species at temperatures up to approximately 15,000 R were molecular oxygen, nitrogen and nitric oxide as well as atomic oxygen and nitrogen. At temperatures greater than about 15,000 R the molecular species dissociate, thus the composition at higher temperatures is dominated by atomic oxygen and nitrogen, electrons and the positive ions of oxygen and nitrogen.

Major contributors to the seed gas opacity in the ultraviolet spectral region above a wave number of 33,000 cm^{-1} include the Herzberg continuum, Schumann-Runge continuum and bands and the Hopfield bands of oxygen, the Hopfield bands of nitrogen, the Lyman-Birge-Hopfield bands, several sharp bands including the β , γ , δ and ϵ transitions and the ionization continuum of nitric oxide (see Ref. 13). Atomic and ionic species contribute various bound-free and free-free continua to the spectral absorption coefficients throughout the spectrum (Refs. 14 and 15).

Density Profiles

The composition data required to compute the spectral absorption coefficient distributions for cases 1 through 6 were used to calculate nuclear fuel and total mass density profiles as a function of axial or radial position within the outer layer of the fuel-containment region. Nuclear fuel mass density distributions for each of the cases studied during this investigation are compared in Fig. 10 for cases 1 and 2, in Fig. 11 for cases 1 and 3, in Fig. 12 for cases 1, 4 and 5 and in Fig. 13 for cases 1, 4 and 6. Similarly, total mass density profiles are compared in Fig. 14 for cases 1 and 2, in Fig. 15 for cases 1 and 3, in Fig. 16 for cases 1, 4 and 5 and in Fig. 17 for cases 1, 4 and 6. The total density is defined as the sum of the densities of all gas species present: nuclear fuel, seed gases and neon.

Spectral Radiative Energy Profiles

Spectral distributions of the radiative flux emitted from the nuclear fuel containment region of a typical unit cavity (see Fig. 1) of a nuclear light bulb engine are graphically shown in Figs. 18, 20, 22 and 24 for all cases investigated. The spectral radiative flux distributions for a black body at a temperature of 15,000 R are also shown in Figs. 18, 20, 22 and 24 for comparison purposes. In Figs. 19, 21, 23 and 25 the spectral radiative flux results are replotted as fractional flux distributions. Fractional flux results give the fraction of total energy radiated in the wave number interval between 1.0×10^3 cm^{-1} and ω and in the wave number interval between ω and 1.0×10^6 cm^{-1}. Fractional flux distributions for a black body at temperatures of 10,000 R, 15,000 R and 20,000 R are also shown in Figs. 19, 21, 23 and 25. As noted previously, the total radiated flux was 24,300 Btu/ft^2-sec for cases 1, 3, 4, 5 and 6 and 48,600 Btu/ft^2-sec for case 2. The corresponding effective black-body radiating temperatures for these total fluxes are 15,000 R and 17,838 R.

Effect of Doubling Total Radiated Flux on Radial Spectral Flux Distribution

In cases 1 and 2, the effect of doubling the total radiated flux on the spectral distribution of energy emitted radially from the fuel region was investigated. Both cases were calculated using pure nuclear fuel without seed gases. The total radiated flux for case 1 was 24,300 Btu/ft^2-sec, corresponding to an effective black-body radiating temperature of 15,000 R; the total radiated flux for case 2 was 48,600 Btu/ft^2-sec, corresponding to an effective black-body radiating temperature of 17,838 R.

Spectral radiative flux distributions for cases 1 and 2 as well as similar results for a black body at a temperature of 15,000 R are graphically compared in Fig. 18 as a function of wave number. The results shown in Fig. 18 for cases 1 and 2 exhibit approximately the same wave number dependence. (Since the total energy radiated in case 2 was twice that radiated in case 1, the spectral flux for case 2 exceeds the spectral flux for case 1 at all wave numbers.) The spectral results shown in Fig. 18 are displayed in Fig. 19 as fractional flux distributions. Since the transparent walls of the nuclear light bulb engine become essentially opaque at wave numbers greater than approximately 55,000 cm^{-1}, it is significant that the fraction of total energy radiated in this wave number region increases from approximately 17 percent to about 19.5 percent for a two-fold increase in total radiated energy. Thus the need for the addition of seed material increases with increasing radiated flux.

Effect of an Oxygen-Nitric Oxide Seed Mixture on Radial Spectral Flux Distribution

Previous studies (Ref. 2) illustrated that seeding the fuel region could reduce the fraction of total energy radiated in the critical wave number region beginning at a wave number of about 55,000 cm^{-1}. These investigations showed that hydrogen as a seed gas effectively eliminated radiation of energy at wave numbers greater than approximately 105,000 cm^{-1} due to absorption of energy by the Lyman-continuum of atomic hydrogen. Unfortunately, the hydrogen does not absorb appreciably between wave numbers of 55,000 cm^{-1} and 105,000 cm^{-1} except for a negligible spectral region centered about a wave number of 82,000 cm^{-1}. Absorption by atomic hydrogen at 82,000 cm^{-1} is due to the Lyman-α line transition. Studies were made during the present investigation to find a suitable gas or combination of gases which would function as an effective absorber in the critical wave number region. Preliminary results indicated that materials such as lithium vapor, oxygen and nitrogen would not provide sufficient opacity in the wave number region above 55,000 cm^{-1}. These studies also indicated that relatively modest quantities of a mixture of oxygen and nitric oxide would be sufficiently stable at the conditions of pressure and temperature occurring in the outermost layer of the fuel region and would be sufficiently opaque to radiation at wave numbers greater than 55,000 cm^{-1} to function as an effective seed mixture. Thus, a mixture of 5 atm each of oxygen and nitric oxide were used as a seed mixture in case 3. The spectral distribution of energy emitted from the fuel region for case 3 (with oxygen-nitric oxide seeding) are compared to similar results for case 1 (without seeding) in Fig. 20. These estimates of the spectral flux distributions show that the oxygen-nitric oxide seed mixture blocks essentially all energy radiated at wave numbers greater than about 50,000 cm^{-1}. The curve for case 3 in Fig. 20 also shows that the spectral flux at wave numbers greater than approximately 50,000 cm^{-1} is effectively reduced below that of a black body at a temperature of 15,000 R.

The fractional fluxes for cases 1 and 3 as well as fractional flux results for black-bodies at temperatures of 10,000, 15,000 and 20,000 R are plotted in Fig. 21. These results show that less than 0.4 percent of the total energy radiated by the seeded fuel occurs at wave numbers greater than 55,000 cm^{-1}.

Effect of Reflective End Walls on Axial Spectral Flux Distribution

Reflection of axially directed radiation back into the fuel-containment region is ostensibly a simple means of minimizing end-wall heat loads in the full-scale engine. A perfectly reflecting end-wall (100 percent reflection of radiation at all wavelengths or wave numbers) would preclude deposition of radiation in the end wall and force the fuel region to radiate all energy radially toward the transparent containment wall. Unfortunately, real materials are generally poor reflectors in the ultraviolet region of the electromagnetic spectrum. For a given total net radiative flux incident on a typical reflecting wall, the gas temperature is considerably greater than the gas temperature for a non-reflecting wall (see Fig. 4). For a reflecting wall to be effective in minimizing heat deposition in the end wall, it must effect a significant increase in the fraction of the flux directed radially, not simply an increase in gas temperature. To properly evaluate radiative transport in the end-wall region requires a two-dimensional analysis which includes the effects of reflection. Because of the mathematical complexity of this type of analysis, it would be of benefit to assess the feasibility of defining a "mean" or "effective" reflectance which could be incorporated into a simplified diffusion analysis of the system. As an initial step in evaluating this concept, the effects of reflective end walls in the one-dimensional system with uniform total radiated flux were examined.

The spectral reflectivities of aluminum in case 4 and silver in case 6 (see Fig. 3) were used in the spectral analysis of radiation emitted axially from the fuel region. Spectral radiative flux distributions are compared in Fig. 22 for cases 1, 4 and 5. These spectral results (Fig. 22) show that the distribution of energy is shifted toward wave numbers in the ultraviolet region of the spectrum when reflective end walls are incorporated in the analysis. The ultraviolet shift corresponds to the increase in the temperatures for these cases. Examination of the temperature distributions depicted in Fig. 4 for cases 4 and 5 show that the edge-of-fuel temperatures increase markedly from 10,650 R for case 1 involving no reflective walls to 23,650 R for case 4 involving aluminum end walls and to 17,650 R for case 5 involving silver end walls.

In Fig. 23, the fractional flux distributions for cases 1, 4 and 5 and for a black body at temperatures of 10,000 R, 15,000 R and 20,000 R are compared. In general, these results show that reflective end walls tend to shift the flux distribution such that more of the emitted energy falls in the visible and ultraviolet spectral regions.

Effect of Reflective End Walls with Seeding on Axial Spectral Flux Distribution

In case 6, the effect on the axially emitted spectral flux distribution of adding 5 atm of oxygen and 5 atm of nitric oxide as a seeding mixture to a fuel region bounded by aluminum end walls was studied. The spectral flux distribution for case 6 is compared to the spectral flux distributions for case 1 (no seeds or reflective end walls) and case 4 (no seeds and reflective end walls of aluminum) in Fig. 24. Corresponding fractional flux distributions for cases 1, 4 and 6 are compared in Fig. 25. These results show some attenuation of the ultraviolet radiation when an oxygen-nitric oxide seed mixture is used. However, the absorption coefficients of this seed mixture (see Figs. 8 and 9) at the higher temperatures encountered in the reflective end wall case (case 6) are not great enough to substantially reduce radiation of energy in the ultraviolet spectral region.

Optical Depths at Selected Wave Number

In order to ascertain the thickness of fuel which influences the spectral radiation flux at the edge of fuel, it is necessary to know the "effective" optical depth. The optical depth at any wave number is given by the following equation:

$$\tau_\omega = \int_0^y a_\omega \, dy \qquad (1)$$

where y is the distance from the fuel edge and a_ω is the spectral absorption coefficient as a function of y. Spectral absorption coefficient data, such as those given in Figs. 5 through 9, were used to compute the optical depths as a function of distance into the fuel for each of the cases investigated at wave numbers of 2.0×10^3, 1.0×10^4, 2.0×10^4, 5.0×10^4 and 1.0×10^5 cm^{-1}. These results are graphically illustrated in Figs. 26 through 31 for cases 1 through 6 respectively.

In practice, the spectral flux of radiative energy emitted by the fuel region is not appreciably influenced by conditions existing more than a few optical depths into the interior of the fuel-containment region as shown by the results of this section. An optical depth of 1.0 is generally reached or exceeded at wave numbers of 10,000, 20,000, 50,000 and 100,000 cm^{-1} at a position within approximately 0.6 cm of the edge of fuel. Figures 29 and 31 show that the optical depth criterion for cases 4 and 6 at a wave number of 10,000 cm^{-1} is not met at all positions within the fuel region; however, the fraction of radiation emitted up to a wave number of 10,000 cm^{-1} for cases 4 and 6 is less than 2 percent (see Fig. 25). Although there is a marked reduction in the optical depth at wave numbers less than 2,000 cm^{-1} at all positions within the fuel region for cases 1 though 5, the fraction of radiation emitted at these wave numbers is negligible for all cases (see Figs. 19, 21, 23 and 25).

Effective Spectral Black-Body Properties of the Fuel Region

In Fig. 32 black-body fluxes are illustrated as a function of temperature for selected wave numbers. These results were used to estimate the effective spectral black-body radiating temperature $T_{bb}(\omega)$, of the nuclear fuel region as a function of wave number as graphically depicted in Fig. 33 for all six cases investigated. The effective spectral black-body radiating temperature is defined as that temperature for which the spectral flux emitted by the fuel region at wave number ω is equal to a black-body spectral flux at wave number ω.

A number of general trends are observed in the results presented in Fig. 33. In the infrared spectral region (nominally at wave numbers less than 13,000 cm^{-1}) the fuel systems for cases 1, 2 and 3 which do not involve wall reflectivities radiate at black body temperatures greater than 15,000 R. Conversely, in cases 4, 5 and 6 incorporation of reflecting end walls drastically reduces the effective spectral black-body radiating temperatures considerably below 15,000 R. In all cases examined, the effective spectral black-body radiating temperature of the fuel region tends to oscillate around 15,000 R, throughout the visible and near ultraviolet regions of the spectrum. In addition, radiation from fuel systems for all cases except case 3 tends to peak at an effective black-body radiating temperature of 17,500 R at a wave number of approximately 70,000 cm^{-1}. For case 3, involving the oxygen-nitric oxide seed mixture but no reflective walls, the effective black-body radiating temperature tends to remain at 15,000 R at wave numbers above 70,000 cm^{-1}.

Effective Optical Depths of the Fuel Region

In Fig. 34, the effective optical depth is plotted as a function of wave number. The effective optical depth is defined as that optical depth at which the effective spectral black-body temperature and the gas temperature are equal. It is a measure of the effective distance one can "see" into the plasma.

Note that no data could be calculated for cases 4 and 6 which consider reflective end walls of aluminum. These data were not available since the estimated spectral black-body temperatures (see Fig. 32) at the selected wave numbers were less than the gas temperatures plotted in Fig. 4.

The results plotted in Fig. 34 show that the effective optical depth generally increases with increasing wave number for all cases. A notable exception is exhibited by case 3, in which the effective optical depth decreases markedly with increasing wave number at wave numbers greater than 60,000 cm^{-1}. The results for case 3 reflect the addition of the oxygen-nitric oxide seed gas which becomes quite opaque at wave numbers greater than 60,000 cm^{-1} (see Fig. 6).

REFERENCES

1. McLafferty, G. H. and H. E. Bauer: Studies of Specific Nuclear Light Bulb and Open-Cycle Vortex-Stabilized Gaseous Nuclear Rocket Engines. UARL Report F910093-7, September 1967. Also issued as NASA CR-1030, 1968.

2. Krascella, N. L.: Theoretical Investigation of the Radiant Emission Spectrum from the Fuel Region of a Nuclear Light Bulb Engine. UARL Report H910092-12, October 1969.

3. Krascella, N. L.: Theoretical Investigation of the Spectral Opacities of Hydrogen and Nuclear Fuel. Air Force Systems Command Report RTD-TDR-63-1101 prepared by UARL, November 1963.

4. Krascella, N. L.: Theoretical Investigation of the Opacity of Heavy-Atom Gases. UARL Report D-910092-4, September 1965.

5. Waber, J. T., D. Liberman and D. T. Cromer: Private Communication, Los Alamos Scientific Laboratory, Los Alamos, New Mexico, June 1966.

6. Krascella, N. L.: Theoretical Investigation of the Absorptive Properties of Small Particles and Heavy-Atom Gases. UARL Report E-910092-7, September 1966.

7. Bennett, H. E. et al: Infrared Reflectance of Aluminum Evaporated in Ultra-High Vacuum. Journal of the Optical Society of America, Vol. 53, No. 9, September 1968.

8. Cole, T. T. and F. Openheimer: Polarization by Reflection and Some Optical Constants in the Extreme Ultraviolet. Applied Optics, Vol. 1, 1962.

9. Madden, R. P. et al: On the Vacuum Ultraviolet Reflectance of Evaporated Aluminum Before and During Oxidation. Journal of the Optical Society of America, Vol. 53, No. 5, May 1963.

10. Hass, G. et al: Influence of Purity, Substrate Temperature and Aging Conditions on the Extreme Ultraviolet Reflectance of Evaporated Aluminum. Journal of the Optical Society of America, Vol. 47, No. 12, December 1957.

11. Ehrenreich, H. and H. R. Philipp: Optical Properties of Ag and Cu. Physical Review, Vol. 128, No. 4, November 1962.

12. Taft, E. A. and H. R. Philipp: Optical Constants of S. Rver. Physical Review, Vol. 121, No. 4, February 1961.

13. Sullivan, J. O. and A. C. Holland: A Congeries of Absorption Cross Sections for Wavelengths less than 3000 A^{o}. NASA Contractor Report NASA CR-371, January 1966.

14. Churchill, D. R., B. H. Armstrong and K. G. Mueller: Absorption Coefficients of Heated Air: A Compilation to 24,300 K. Journal of Quantitative Spectroscopy and Radiative Transfer, Vol. 6, No. 4, July/August 1966.

15. Blake, A. J., J. H. Carver and G. N. Haddad: Photo-absorption Cross-Sections of Molecular Oxygen Between 1250 A^{o} and 2350 A^{o}. Journal of Quantitative Spectroscopy and Radiative Transfer, Vol. 6, No. 4, July/August 1966.

LIST OF SYMBOLS

a_ω	Spectral absorption coefficient, cm^{-1}
P_F	Partial pressure of nuclear fuel, atm
$P_{F,E}$	Partial pressure of nuclear fuel at edge of fuel, atm
Q_T	Total or integrated radiative flux, Btu/ft^2-sec
Q^*	Black body radiative flux for temperature T*, Btu/ft^2-sec
Q_ω	Spectral radiative flux, Btu/ft-sec
Q_ω^{bb}	Black body spectral flux, Btu/ft-sec
r_ω	Spectral reflectivity, dimensionless
T	Temperature, ^oR or ^oK
T_E	Edge-of-fuel temperature, ^oR
T*	Effective black body radiating temperature, ^oR
$T_{bb}(\omega)$	Effective spectral black-body radiating temperature, ^oR
y	Distance from the edge of fuel, cm
λ	Wavelength, microns
ω	Wave number, cm^{-1}
ρ_F	Nuclear fuel mass density, lb/ft^3
ρ_T	Total mass density, lb/ft^3
τ_ω	Optical depth, dimensionless
$\tau_{\omega,E}$	Effective optical depth, dimensionless

TABLE I

INPUT DATA AND LIST OF FIGURES SHOWING RESULTS OF VARIOUS CASES INVESTIGATED

CASE	INPUT DATA				ANALYTICAL RESULTS FOR VARIOUS CASES IN FIGURES									
	T^* R	Q^* BTU/FT^2 – SEC	SEED	r_ω (1)	T vs y	a_ω vs ω (2)	$\rho_\pm$ vs y	ρ_T vs y	Q_ω vs ω	FRACTIONAL FLUX vs ω	τ_ω vs y	$Q_\omega{}^{bb}$ vs T	T_{bb} (ω) vs ω	$\tau_{\omega,E}$ vs ω
1	15,000	24,300	———	0	4	5.6 7.8	10, 11 12, 13	14, 15 16, 17	18, 20 22, 24	19, 21 23, 25	26	32	33	34
2	17,838	48,600	———	0	4	5	10	14	18	19	27	32	33	34
3	15,000	24,300	5 ATM – O_2 5 ATM – NO	0	4	6	11	15	20	21	28	32	33	34
4	15,000	24,300	———	ALUMINUM SEE FIG. 3	4	7,8	12, 13	16, 17	22, 24	23, 25	29	32	33	34
5	15,000	24,300	———	SILVER SEE FIG. 3	4	7	12	16	22	23	30	32	33	34
6	15,000	24,300	5 ATM – O_2 5 ATM – NO	ALUMINUM SEE FIG. 3	4	8	13	17	24	25	31	32	33	34

(1) REFLECTIVITY, $r = 0$ – USED FOR CASES WITH RADIAL RADIANT HEAT TRANSFER; REFLECTIVITY FOR ALUMINUM AND SILVER WALLS USED FOR CASES WITH AXIAL RADIANT HEAT TRANSFER (SEE FIG. 3)

(2) FIGURE 9 IS A PLOT OF a_ω vs ω AT VARIOUS TEMPERATURES FOR THE OXYGEN –NITRIC OXIDE SEED MIXTURE.

FIG. 1

UNIT CAVITY OF REFERENCE NUCLEAR LIGHT BULB ENGINE

OVERALL ENGINE EMPLOYS SEVEN UNIT CAVITIES SIMILAR TO CAVITY SHOWN

y MEASURED RADIALLY INWARD FROM EDGE OF FUEL FOR CASES 1 THROUGH 3; AXIALLY FROM EDGE OF FUEL FOR CASES 4, 5 AND 6

ALL DIMENSIONS IN FEET

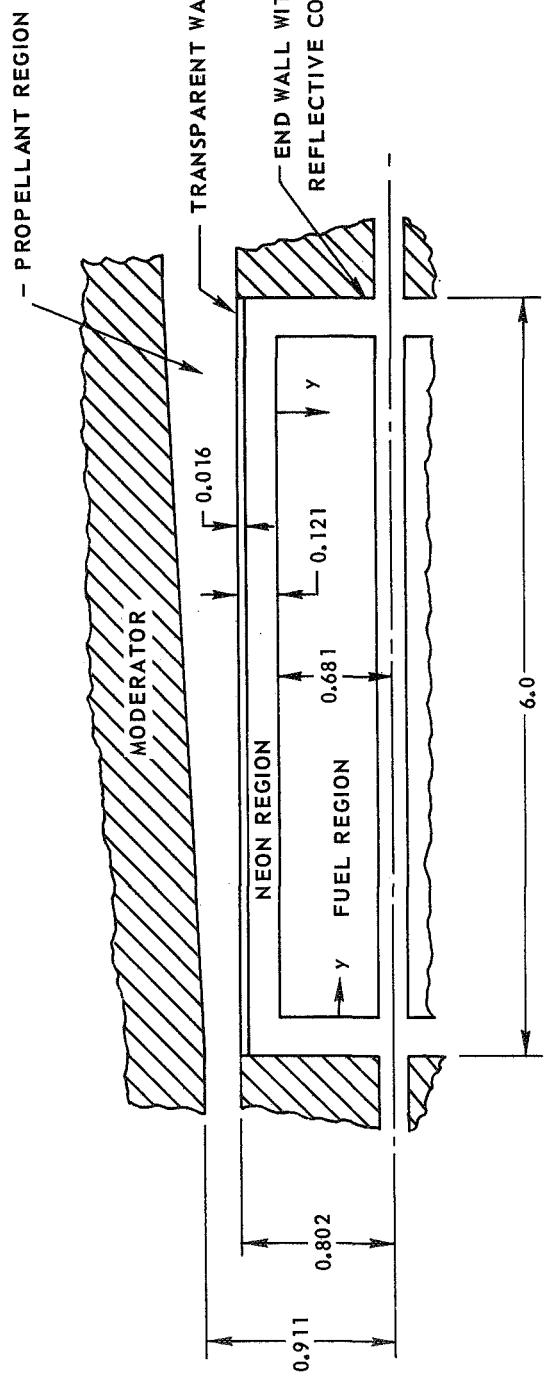

FIG. 2

ASSUMED NUCLEAR FUEL PARTIAL PRESSURE DISTRIBUTION

FOR $y \leq 10{,}378$, $P_F = \begin{cases} 19{,}2698\ y + 0.01 & - \text{CASES 1, 2, 4 AND 5} \\ 19{,}2707\ y & - \text{CASES 3 \& 6} \end{cases}$

FOR $y > 10{,}318$, $P_F = 200$ ATM – ALL CASES

$$P_{FUEL} + P_{SEED} + P_{NEON} = 500 \text{ ATM}$$

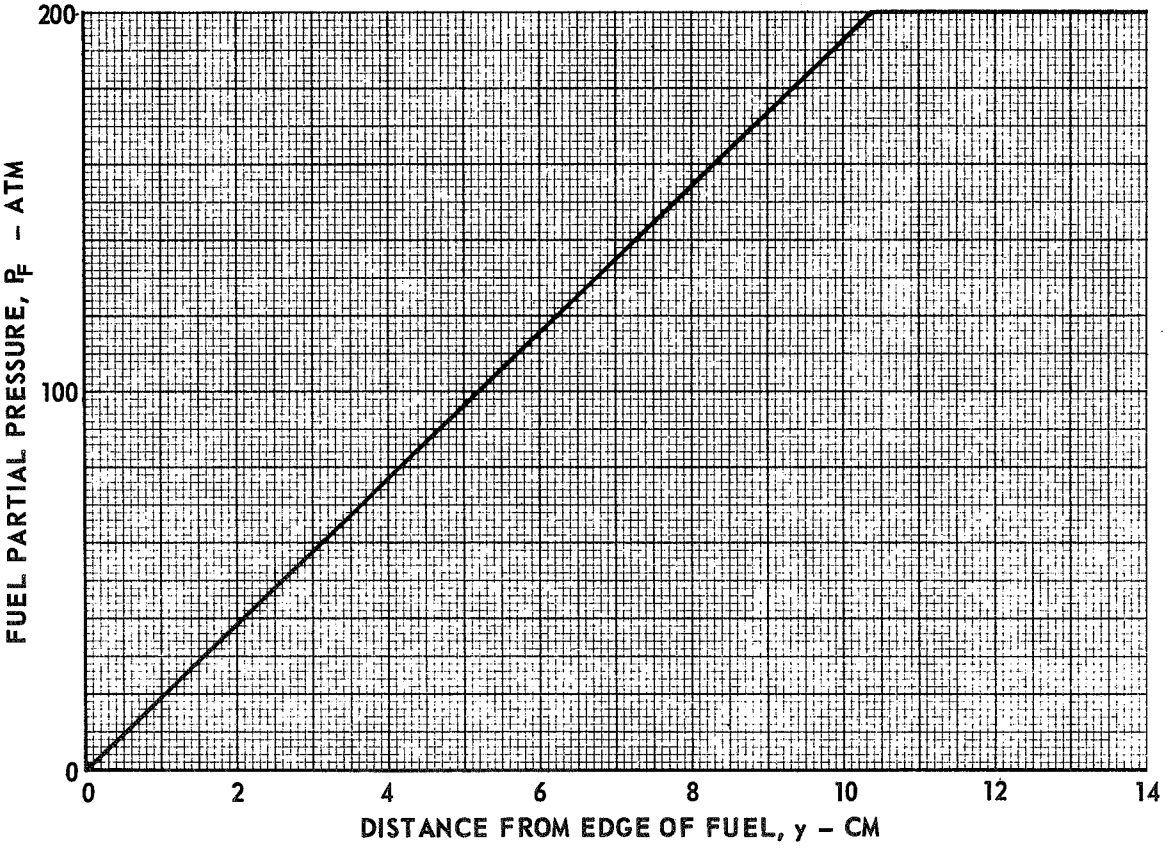

SPECTRAL REFLECTIVITY OF ALUMINUM AND SILVER

CASE & SYMBOL	MATERIAL	REFERENCE
4 & 6 ———	ALUMINUM	7, 8, 9, & 10
5 — — —	SILVER	11 & 12

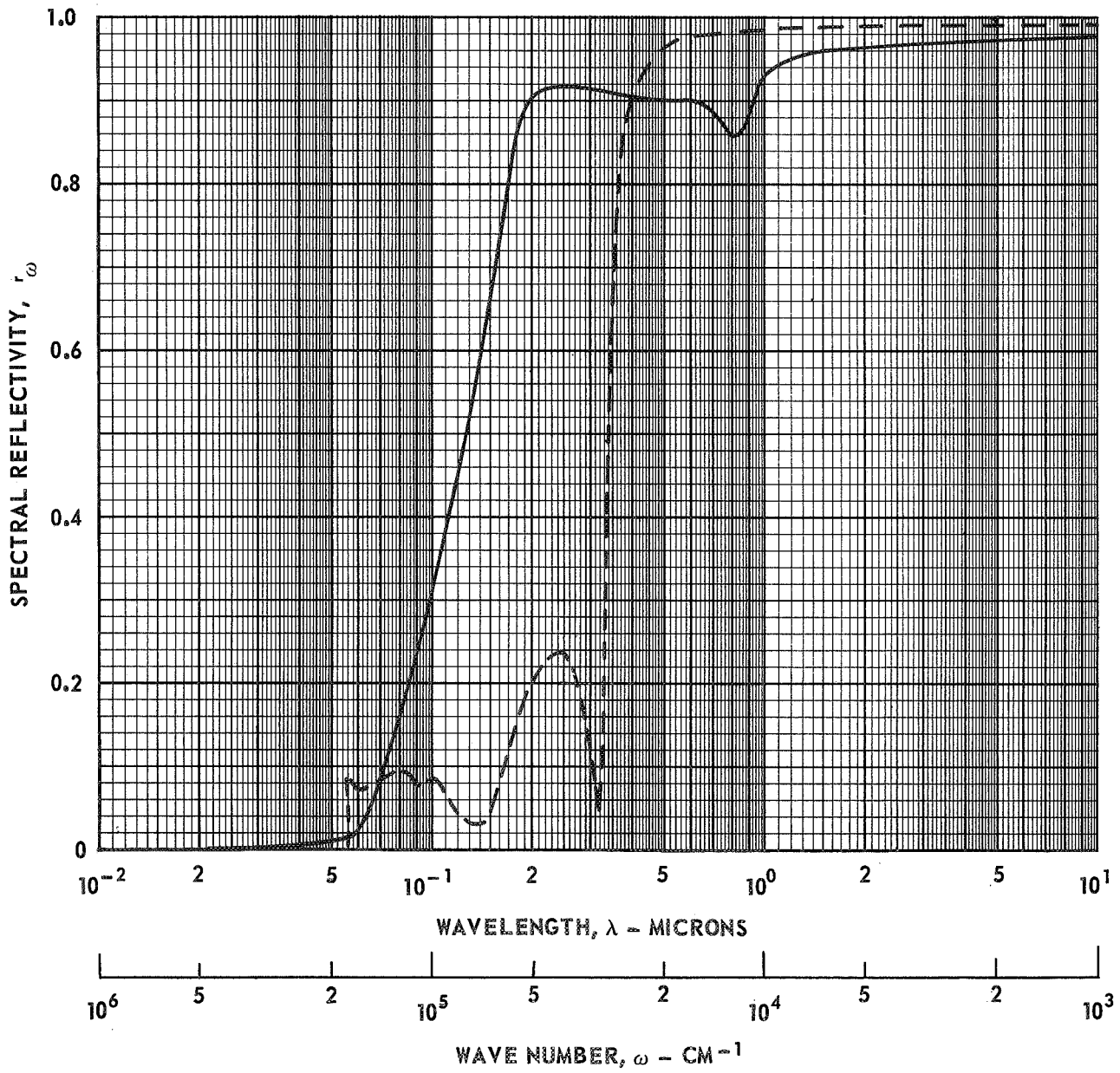

TEMPERATURE DISTRIBUTION IN OUTER LAYER OF FUEL REGION FOR VARIOUS CASES

(CASES INDICATED BY CIRCLED NUMBERS)

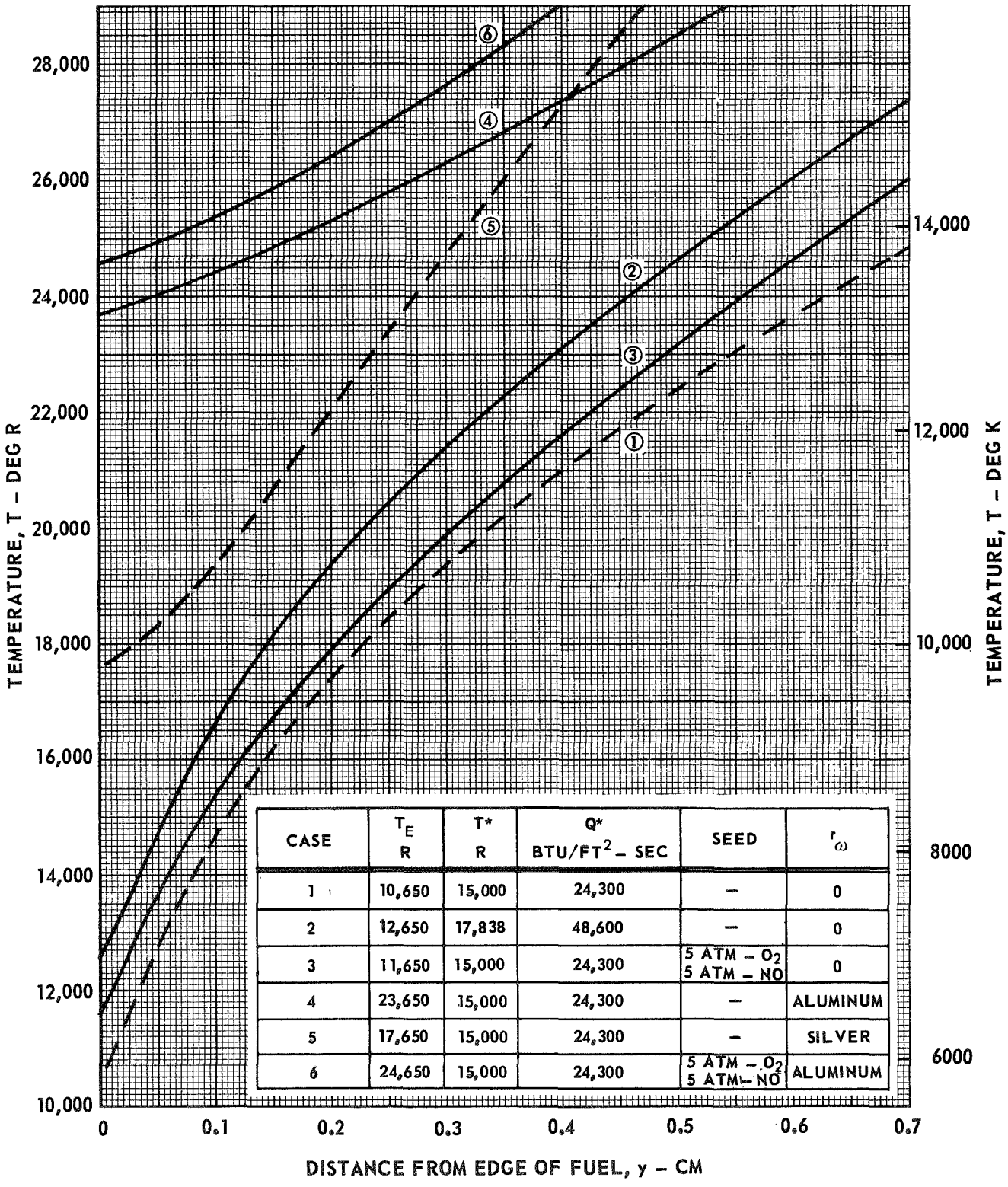

CASE	T_E R	T* R	Q* BTU/FT^2 – SEC	SEED	r_ω
1	10,650	15,000	24,300	–	0
2	12,650	17,838	48,600	–	0
3	11,650	15,000	24,300	5 ATM – O_2 5 ATM – NO	0
4	23,650	15,000	24,300	–	ALUMINUM
5	17,650	15,000	24,300	–	SILVER
6	24,650	15,000	24,300	5 ATM – O_2 5 ATM – NO	ALUMINUM

COMPARISON OF SPECTRAL ABSORPTION COEFFICIENTS OF NUCLEAR FUEL AT EDGE-OF-FUEL TEMPERATURE FOR CASES 1 AND 2

CASE & SYMBOL	T_E R	T* R	Q* BTU/FT^2 – SEC	SEED	r_ω	$P_{F,E}$ ATM
1 ———	10,650	15,000	24,300	—	0	0.01
2 — — —	12,650	17,838	48,600	—	0	0.01

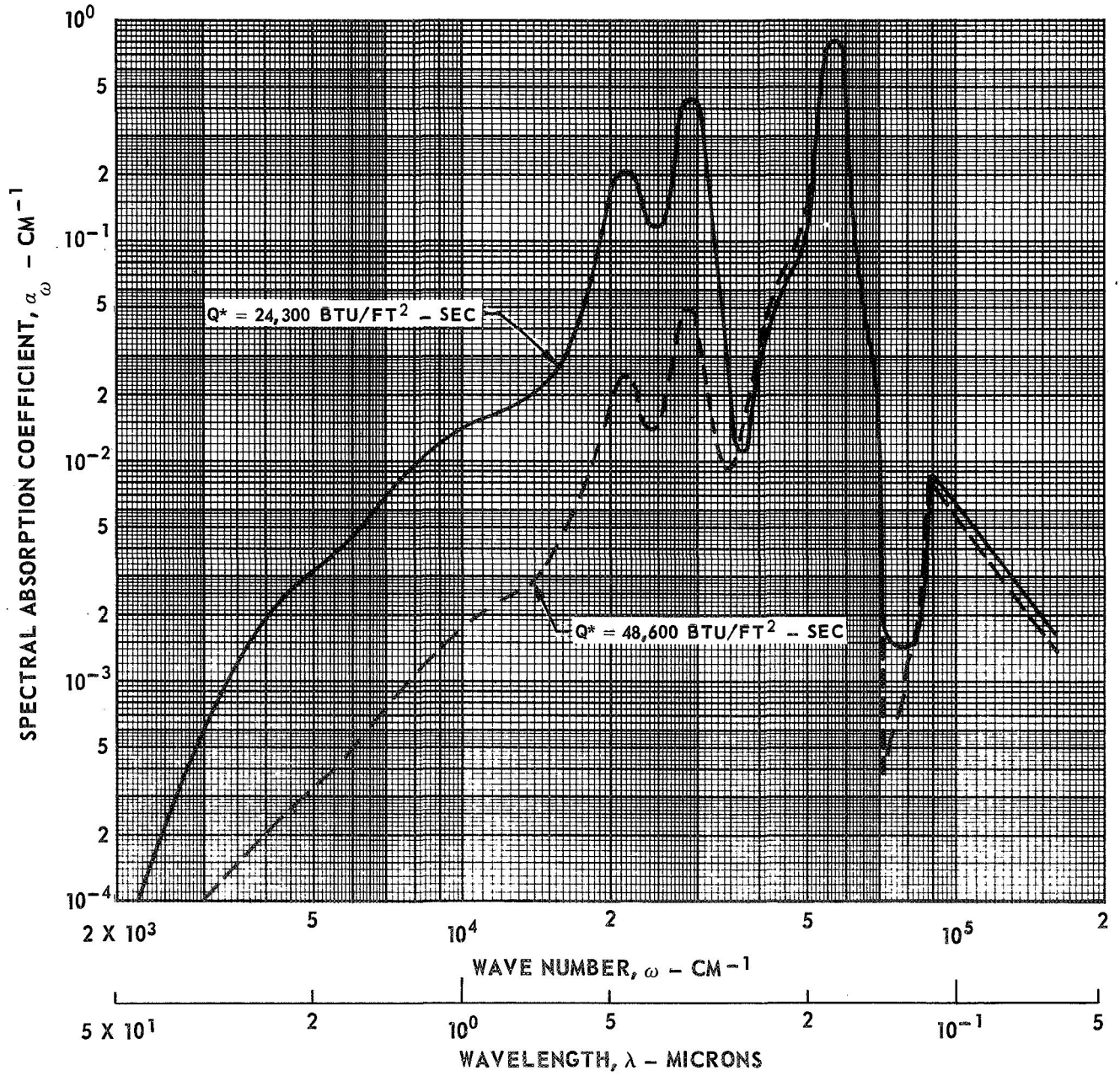

FIG. 6

COMPARISON OF SPECTRAL ABSORPTION COEFFICIENTS OF SEED GASES AND NUCLEAR FUEL AT EDGE - OF - FUEL TEMPERATURE FOR CASES 1 AND 3

CASE & SYMBOL	T_E R	T^* R	Q^* BTU/FT^2 - SEC	SEED	r_ω	$P_{F,E}$ ATM
1 ———	10,650	15,000	24,300	—	0	0.01
3 — — —	11,650	15,000	24,300	5 ATM - O_2 5 ATM - NO	0	0

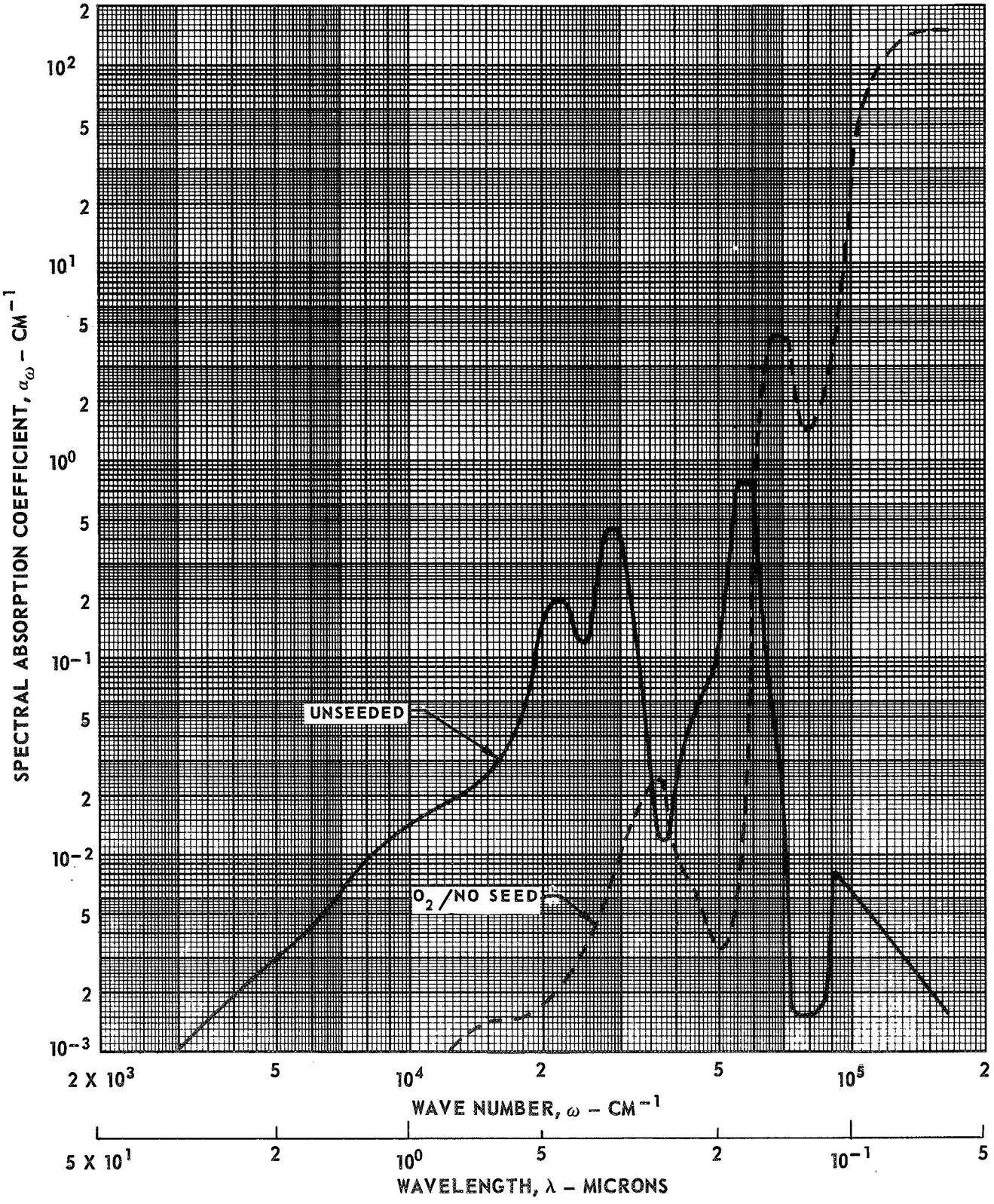

COMPARISON OF SPECTRAL ABSORPTION COEFFICIENTS NUCLEAR FUEL AT EDGE – OF – FUEL TEMPERATURE FOR CASES 1, 4 AND 5

CASE & SYMBOL	T_E R	T* R	Q* BTU/FT^2 – SEC	SEED	r_ω	$P_{F,E}$ ATM
1 ———	10,650	15,000	24,300	—	0	0.01
4 — — —	23,650	15,000	24,300	—	ALUMINUM	0.01
5 ———	17,650	15,000	24,300	—	SILVER	0.01

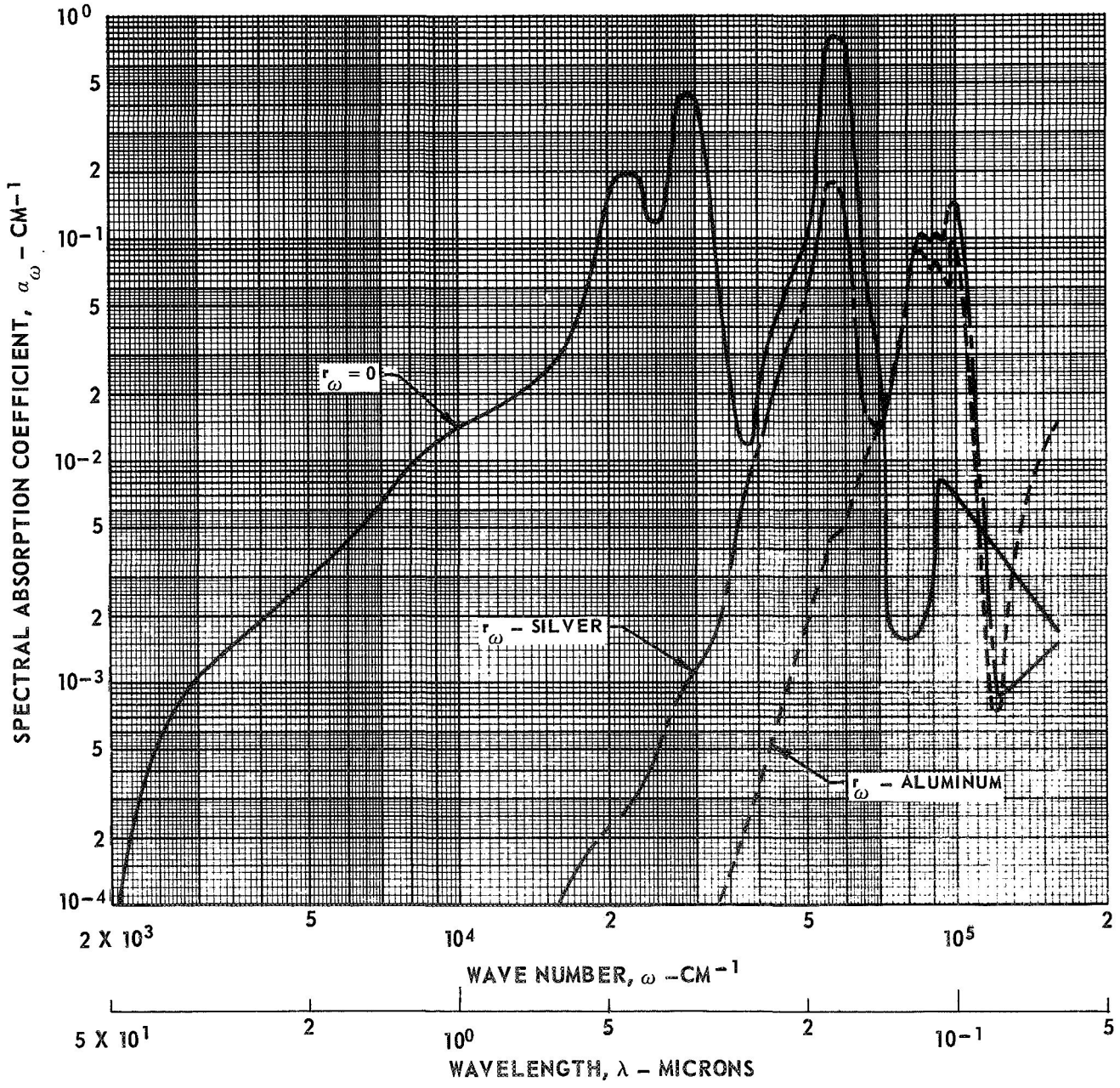

COMPARISON OF SPECTRAL ABSORPTION COEFFICIENTS OF SEED GASES AND NUCLEAR FUEL AT EDGE – OF – FUEL TEMPERATURE FOR CASES 1, 4 AND 6

CASE & SYMBOL	T_E R	T^* R	Q^* BTU/FT^2 – SEC	SEED	r_ω	$P_{F,E}$ ATM
1 ———	10,650	15,000	24,300	—	0	0.01
4 — — —	23,650	15,000	24,300	—	ALUMINUM	0.01
6 —— - ——	24,650	15,000	24,300	5 ATM – O_2 5 ATM – NO	ALUMINUM	0

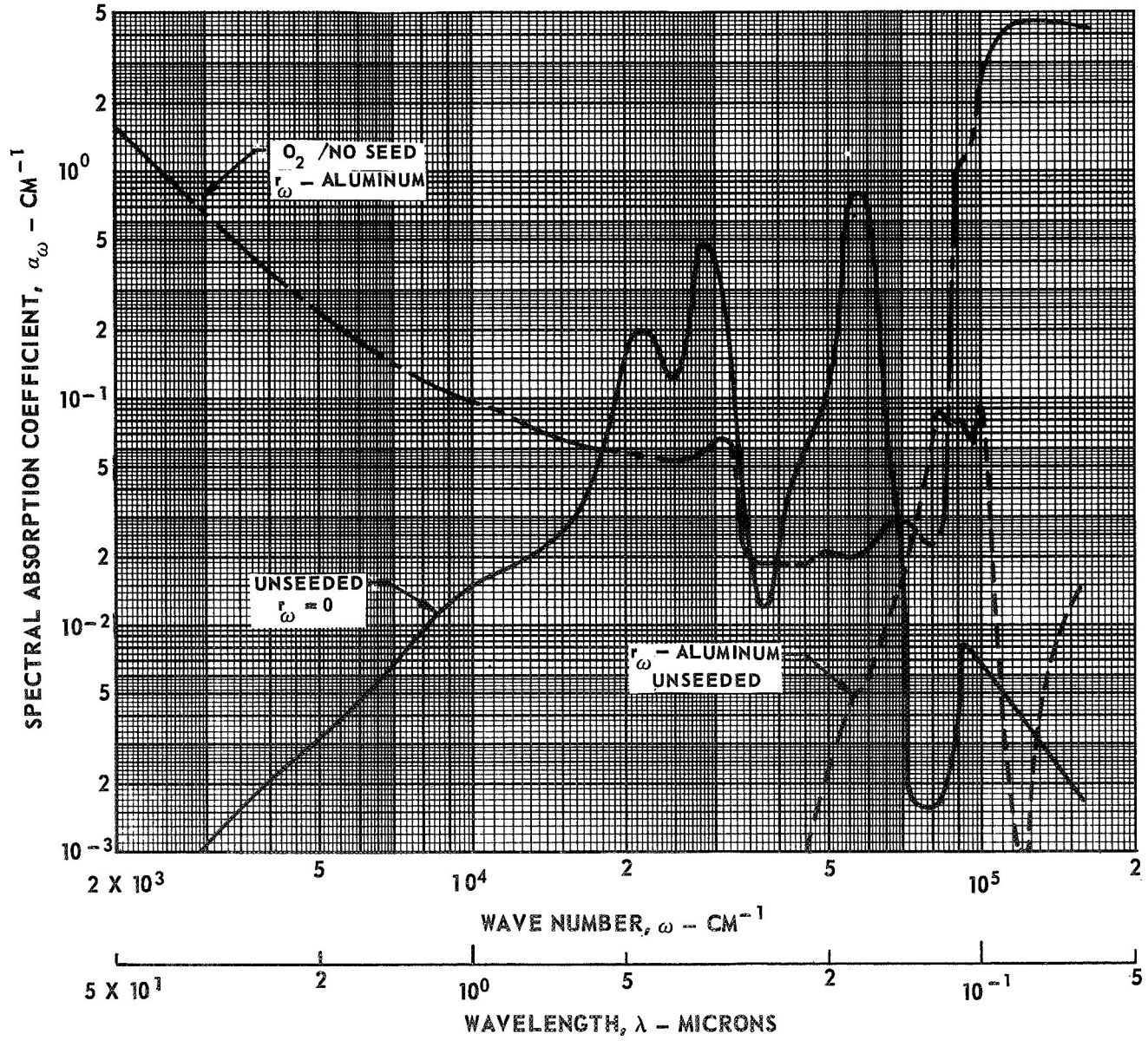

COMPARISON OF SPECTRAL ABSORPTION COEFFICIENT OF OXYGEN – NITRIC OXIDE SEED MIXTURE AT VARIOUS TEMPERATURES

$P_{O_2} = P_{NO} = 5$ ATM

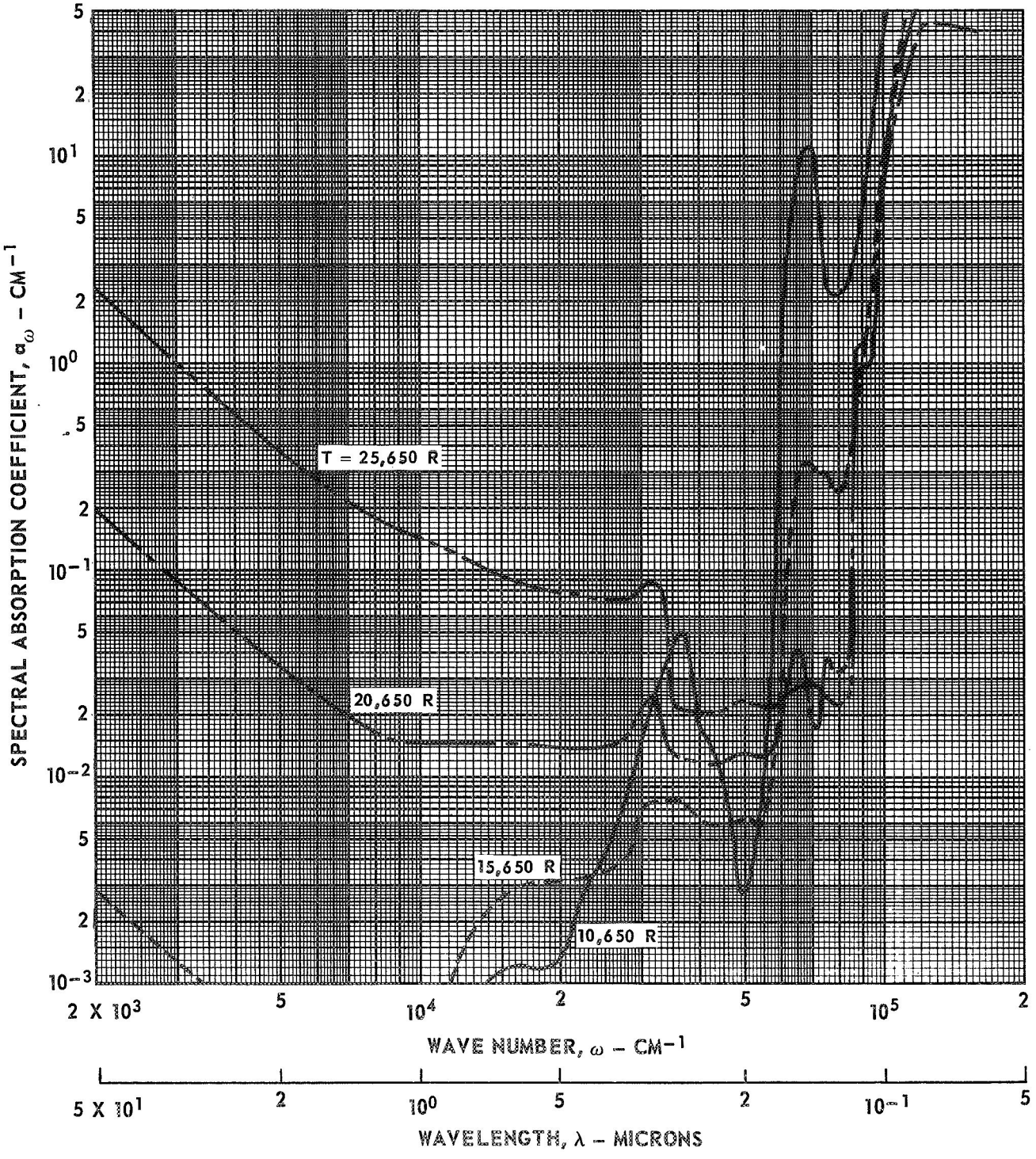

COMPARISON OF NUCLEAR FUEL MASS DENSITY DISTRIBUTIONS FOR CASES 1 AND 2

CASE & SYMBOL	T_E R	T* R	Q* BTU/FT ^{2} – SEC	SEED	r_ω
1 ———	10,650	15,000	24,300	—	0
2 — — —	12,650	17,838	48,600	—	0

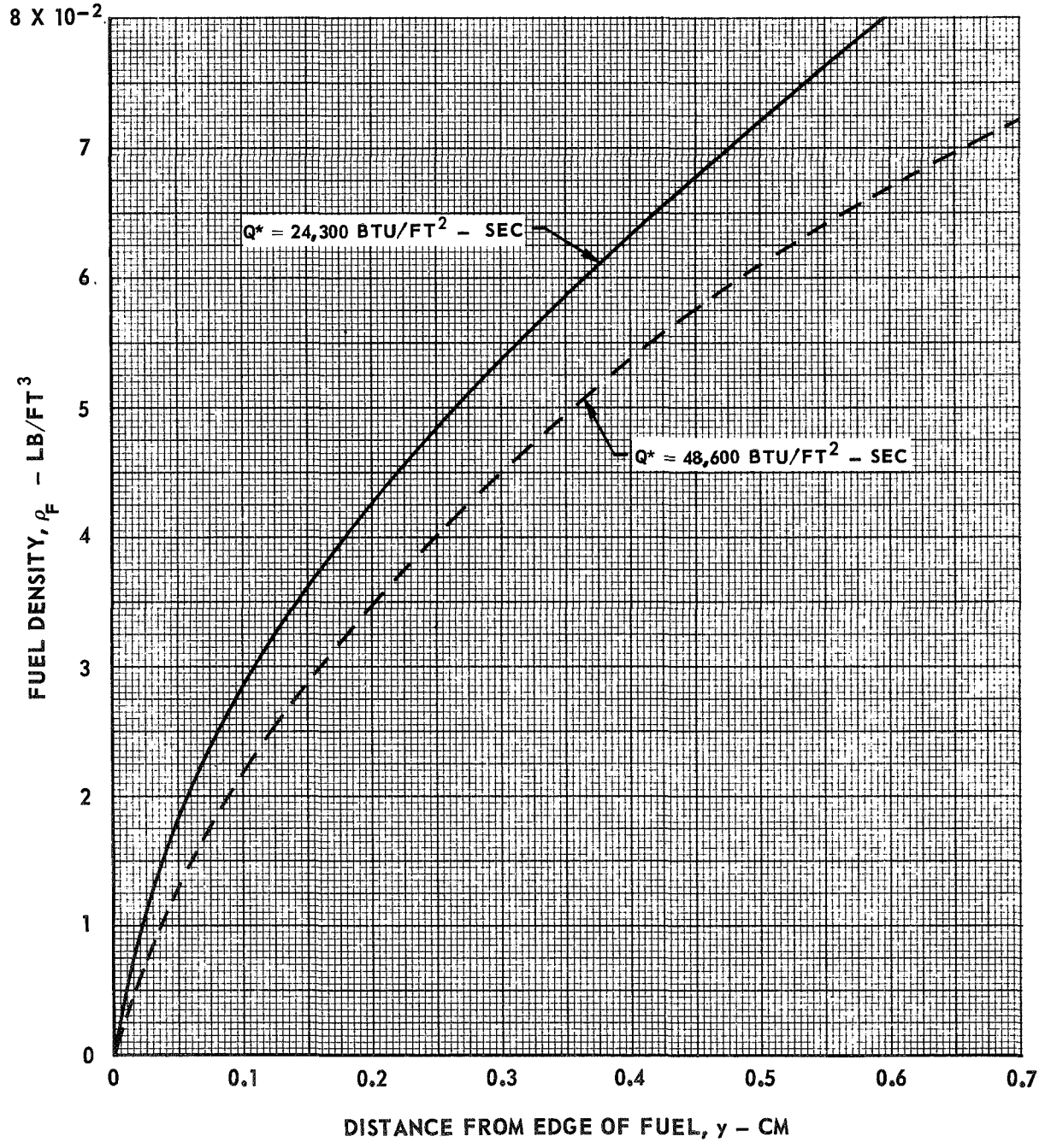

COMPARISON OF NUCLEAR FUEL MASS DENSITY DISTRIBUTIONS FOR CASES 1 AND 3

CASE & SYMBOL	T_E R	T* R	Q* BTU/FT^2 – SEC	SEED	r_ω
1 ———	10,650	15,000	24,300	—	0
3 — — —	11,650	15,000	24,300	5 ATM – O_2 5 ATM – NO	0

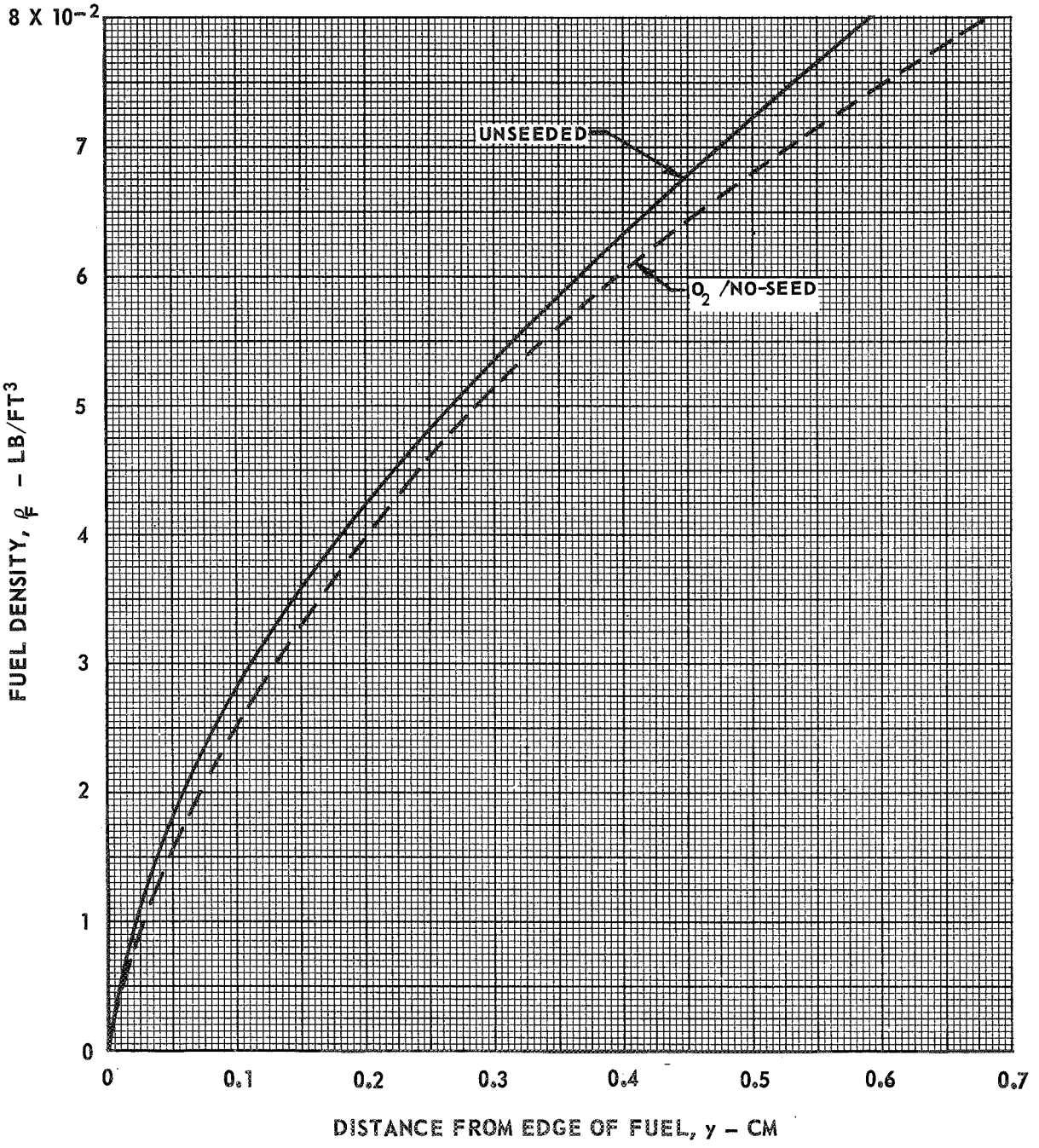

COMPARISON OF NUCLEAR FUEL MASS DENSITY DISTRIBUTIONS FOR CASES 1, 4 AND 5

CASE & SYMBOL	T_E R	T* R	Q* BTU/FT^2 – SEC	SEED	r_ω
1	10,650	15,000	24,300	–	0
4	23,650	15,000	24,300	–	ALUMINUM
5	17,650	15,000	24,300	–	SILVER

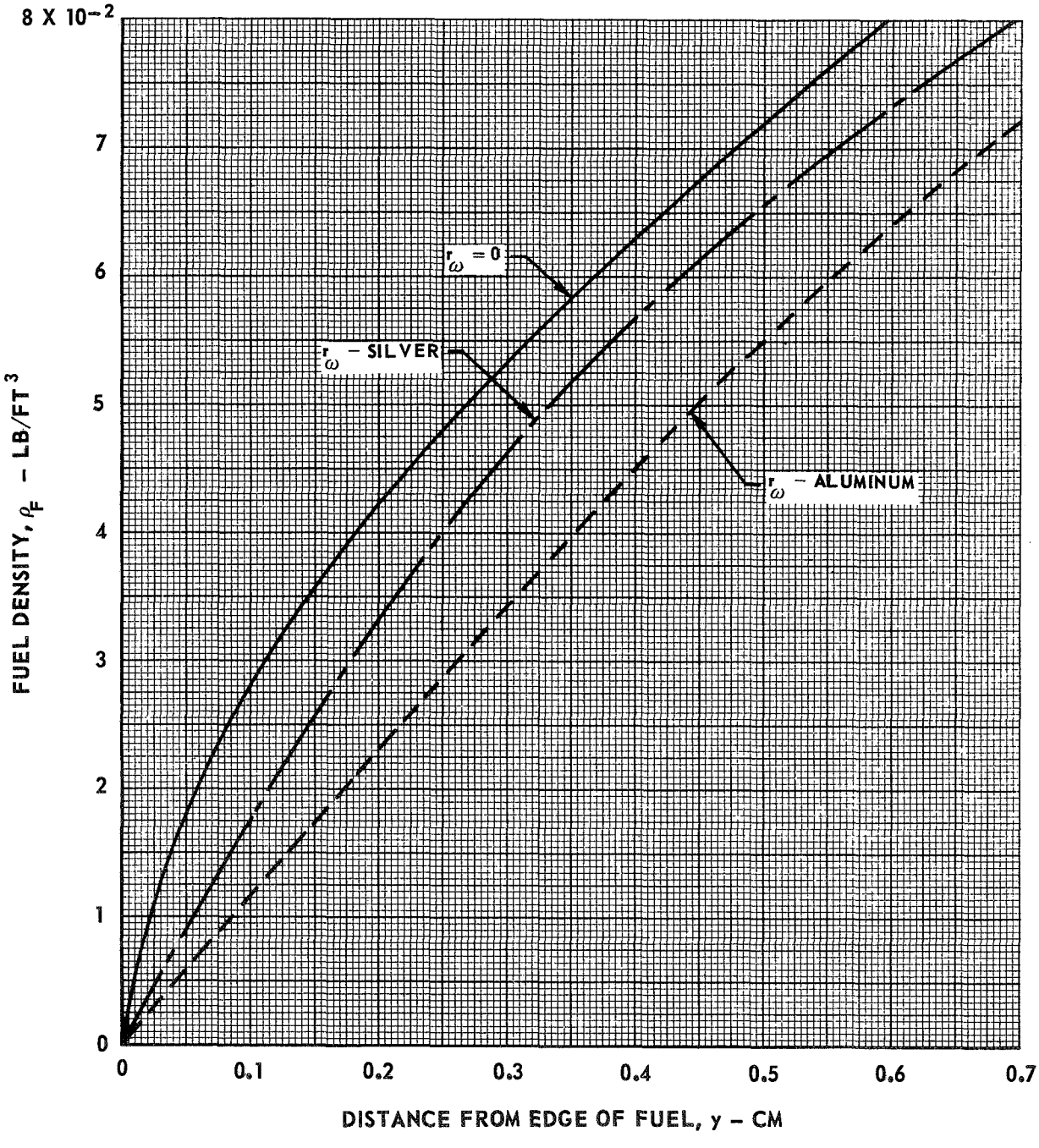

COMPARISON OF NUCLEAR FUEL MASS DENSITY DISTRIBUTIONS FOR CASES 1, 4 AND 6

CASE & SYMBOL	T_E R	T^* R	Q^* BTU/FT^2 – SEC	SEED	r_ω
1 ———	10,650	15,000	24,300	—	0
4 — — —	23,650	15,000	24,300	—	ALUMINUM
6 — - —	24,650	15,000	24,300	5 ATM – O_2 5 ATM – NO	ALUMINUM

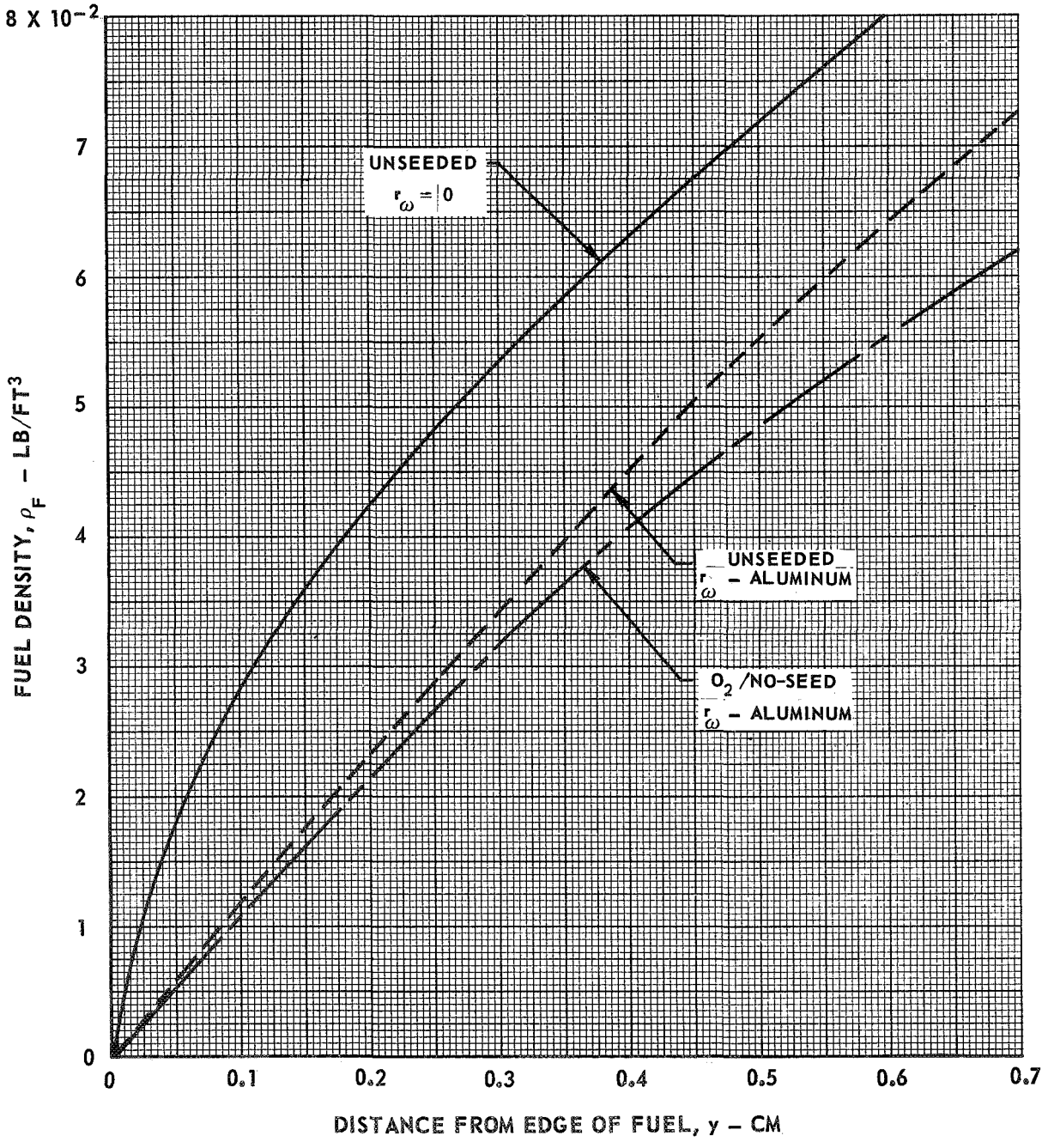

COMPARISON OF TOTAL MASS DENSITY DISTRIBUTIONS FOR CASES 1 AND 2

CASE & SYMBOL	T_E R	T* R	Q* BTU/FT^2 – SEC	SEED	$\dot{r}_\omega$
1 ———	10,650	15,000	24,300	–	0
2 — — —	12,650	17,838	48,600	–	0

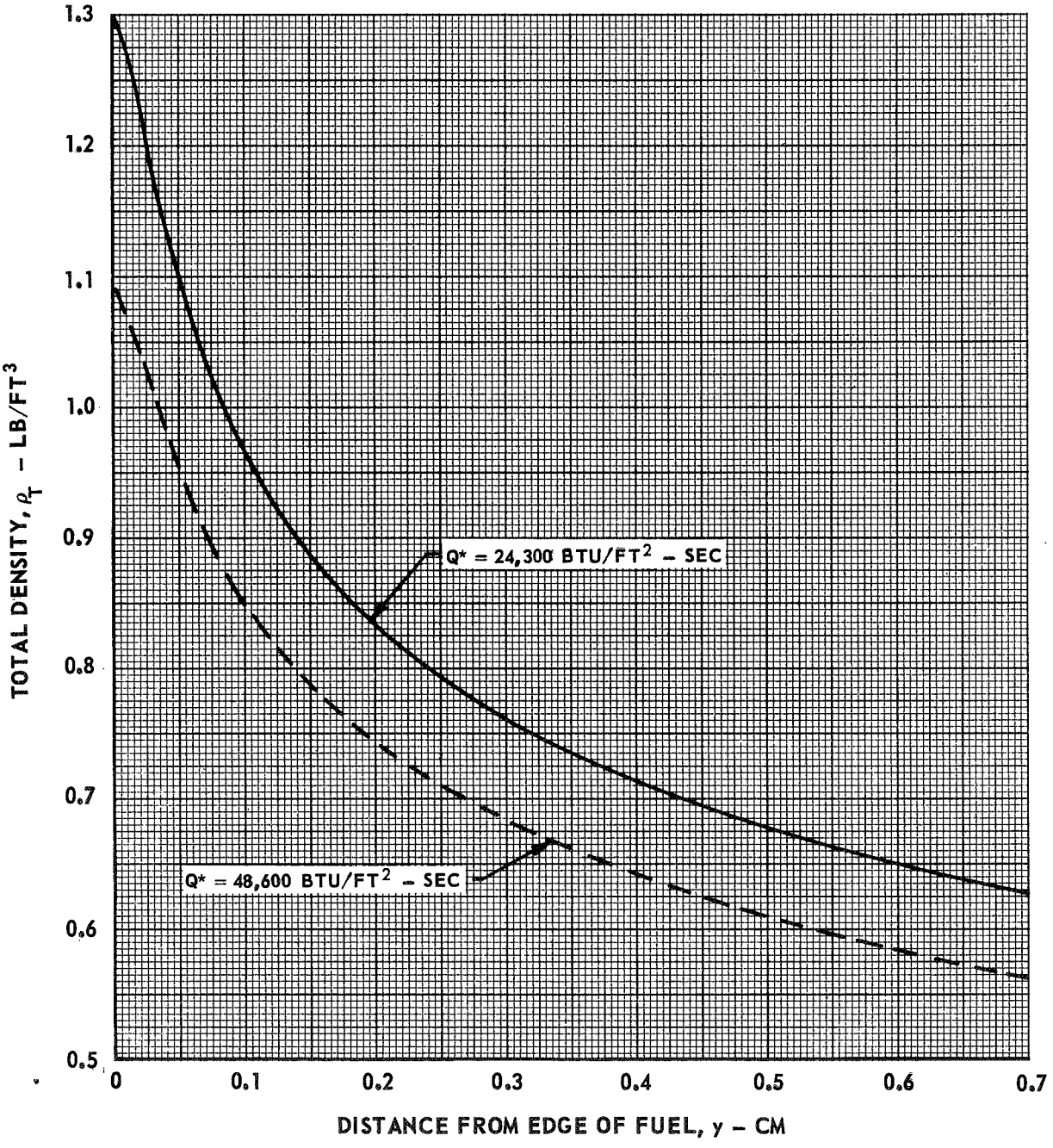

FIG. 15

COMPARISON OF TOTAL MASS DENSITY DISTRIBUTION FOR CASES 1 AND 3

CASE & SYMBOL	T_E R	T^* R	Q^* BTU/FT^2 – SEC	SEED	r_ω
1 ———	10,650	15,000	24,300	—	0
3 — — —	11,650	15,000	24,300	5 ATM – O_2 5 ATM – NO	0

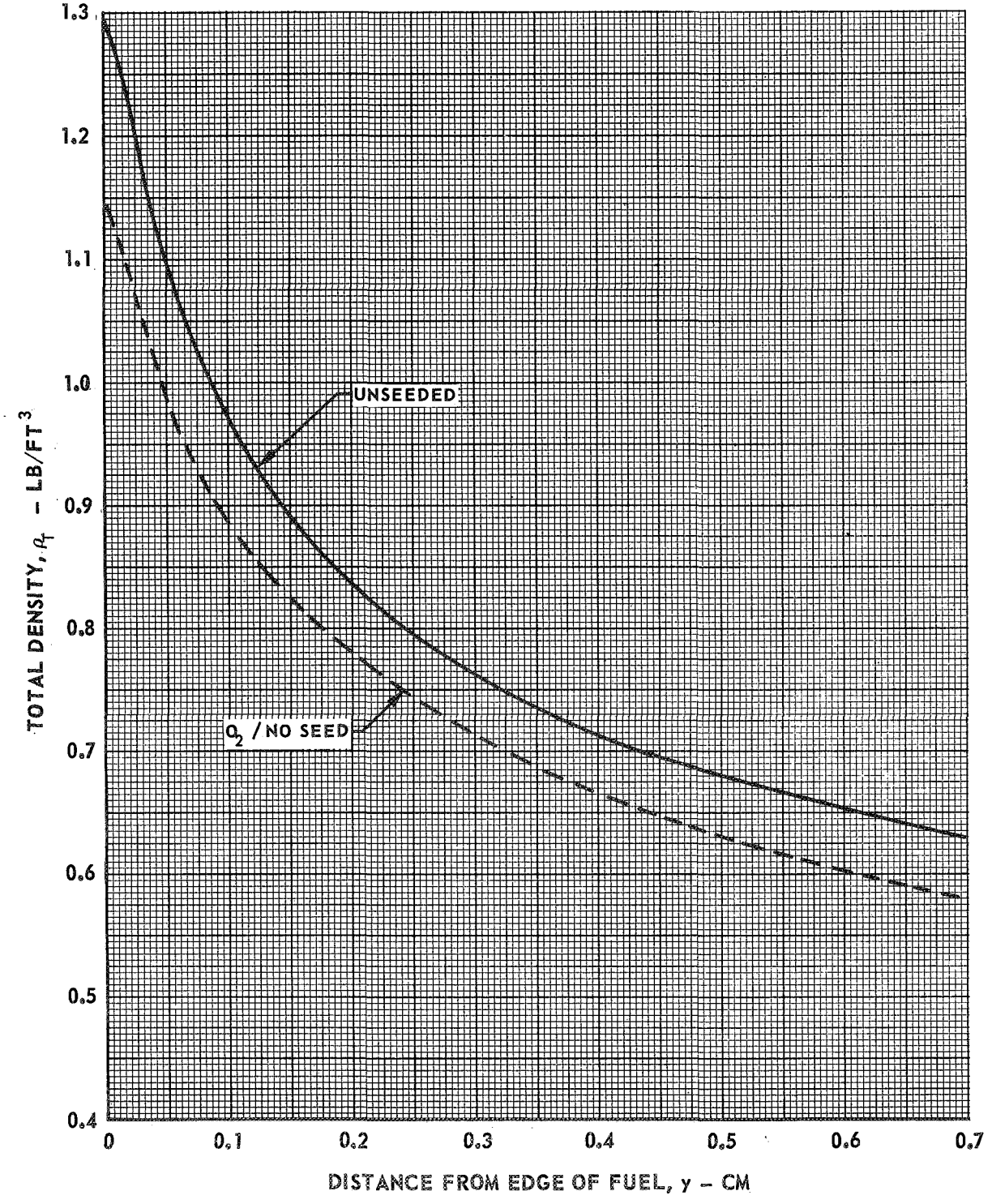

COMPARISON OF TOTAL MASS DENSITY DISTRIBUTIONS FOR CASES 1, 4 AND 5

CASE & SYMBOL	T_E R	T* R	Q* BTU/FT^2- SEC	SEED	r_ω
1 ———	10,650	15,000	24,300	—	0
4 — — —	23,650	15,000	24,300	—	ALUMINUM
5 — - —	17,650	15,000	24,300	—	SILVER

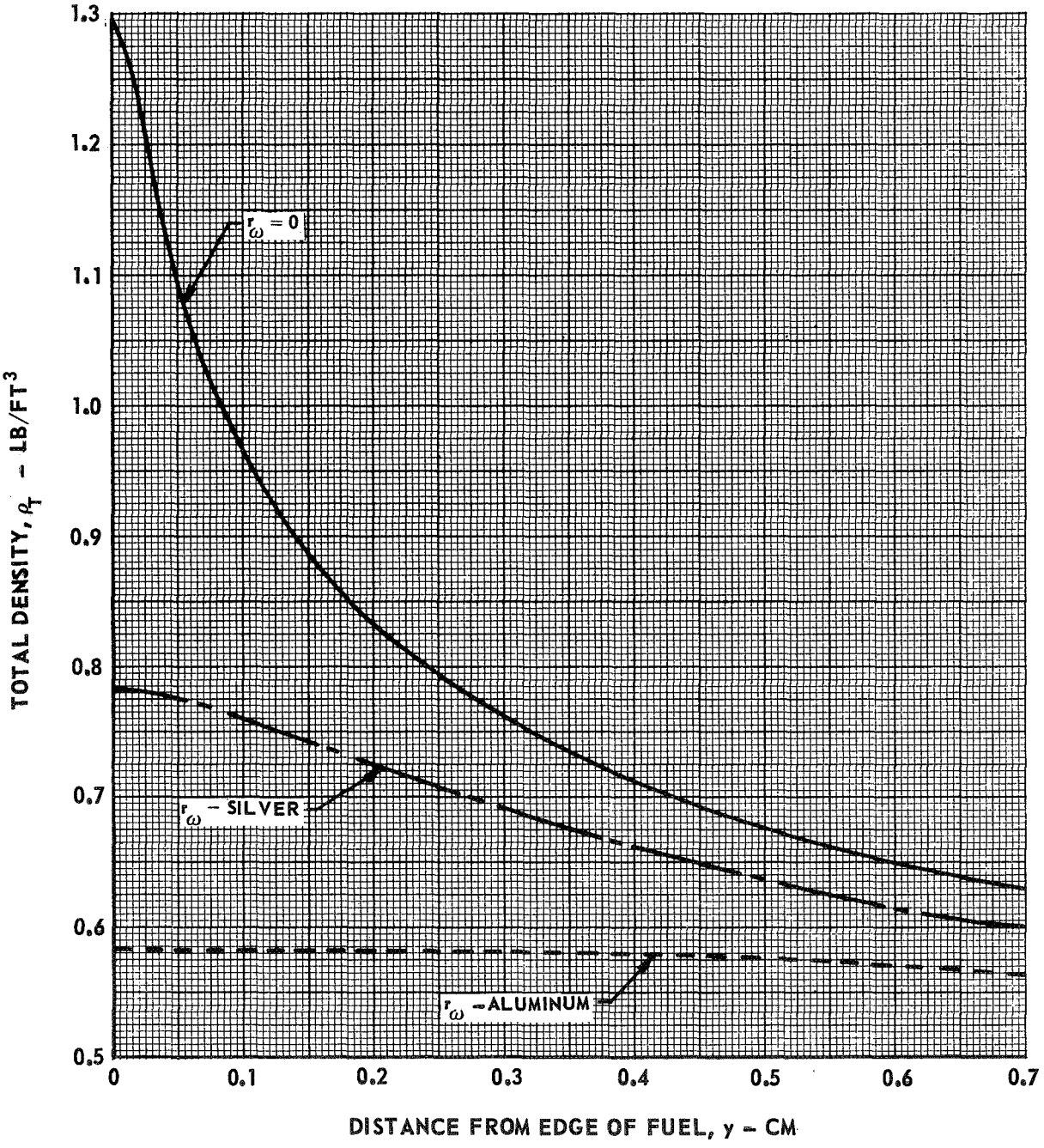

FIG. 17

COMPARISON OF TOTAL MASS DENSITY DISTRIBUTION FOR CASES 1, 4 AND 6

CASE & SYMBOL	T_E R	T* R	Q* BTU/FT^2 – SEC	SEED	r_ω
1 ———	10,650	15,000	24,300	–	0
4 – – –	23,650	15,000	24,300	–	ALUMINUM
6 —·—	24,650	15,000	24,300	5 ATM – O_2 5 ATM – NO	ALUMINUM

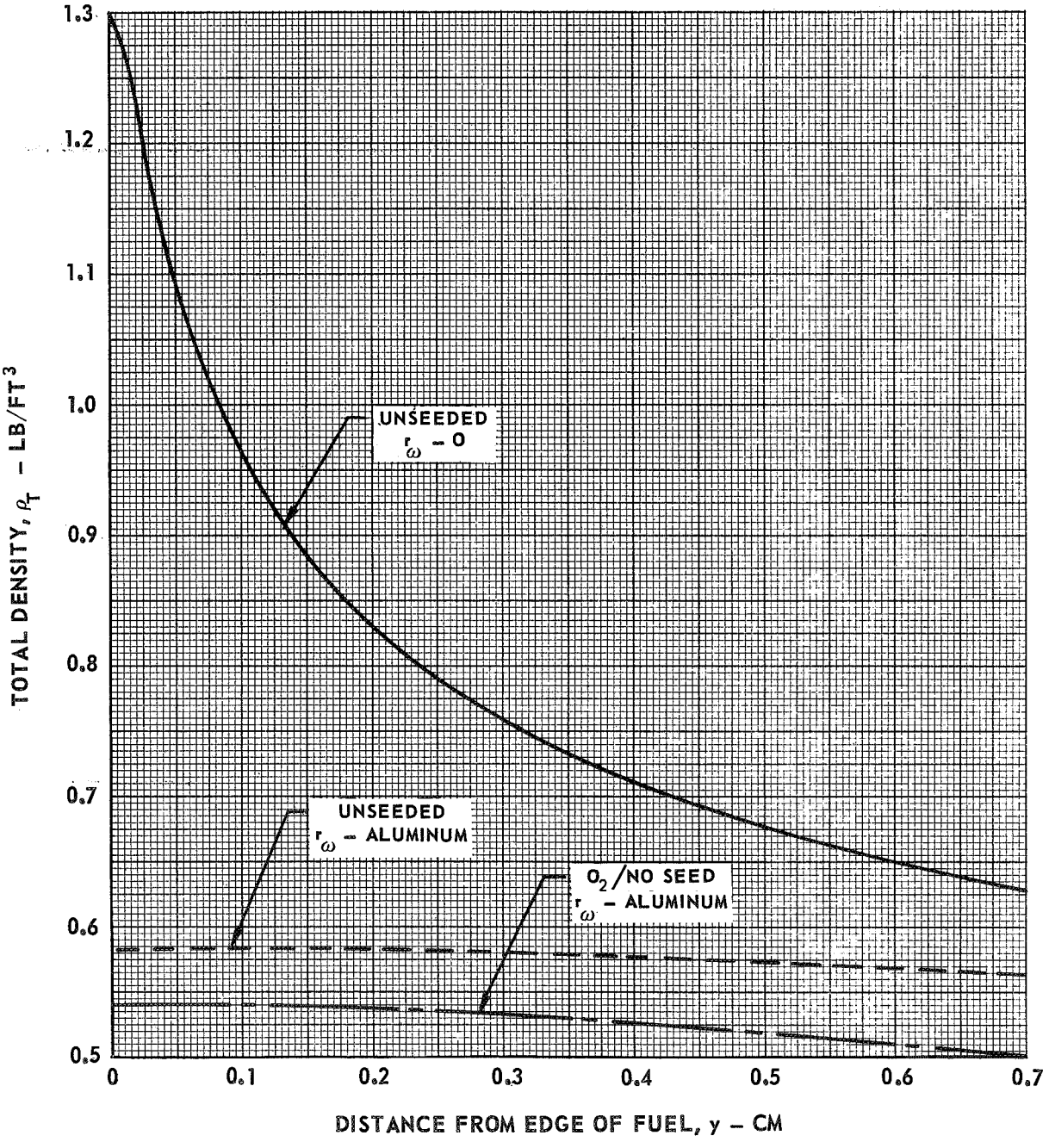

COMPARISON OF SPECTRAL FLUX FOR A BLACK BODY AT A TEMPERATURE OF 15,000 DEG R AND SPECTRAL FLUX EMITTED FROM NUCLEAR FUEL FOR CASES 1 AND 2

CASE & SYMBOL	T_E R	T* R	Q* BTU/FT^2 – SEC	SEED	r_ω
1 ———	10,650	15,000	24,300	—	0
2 – – –	12,650	17,838	48,600	—	0

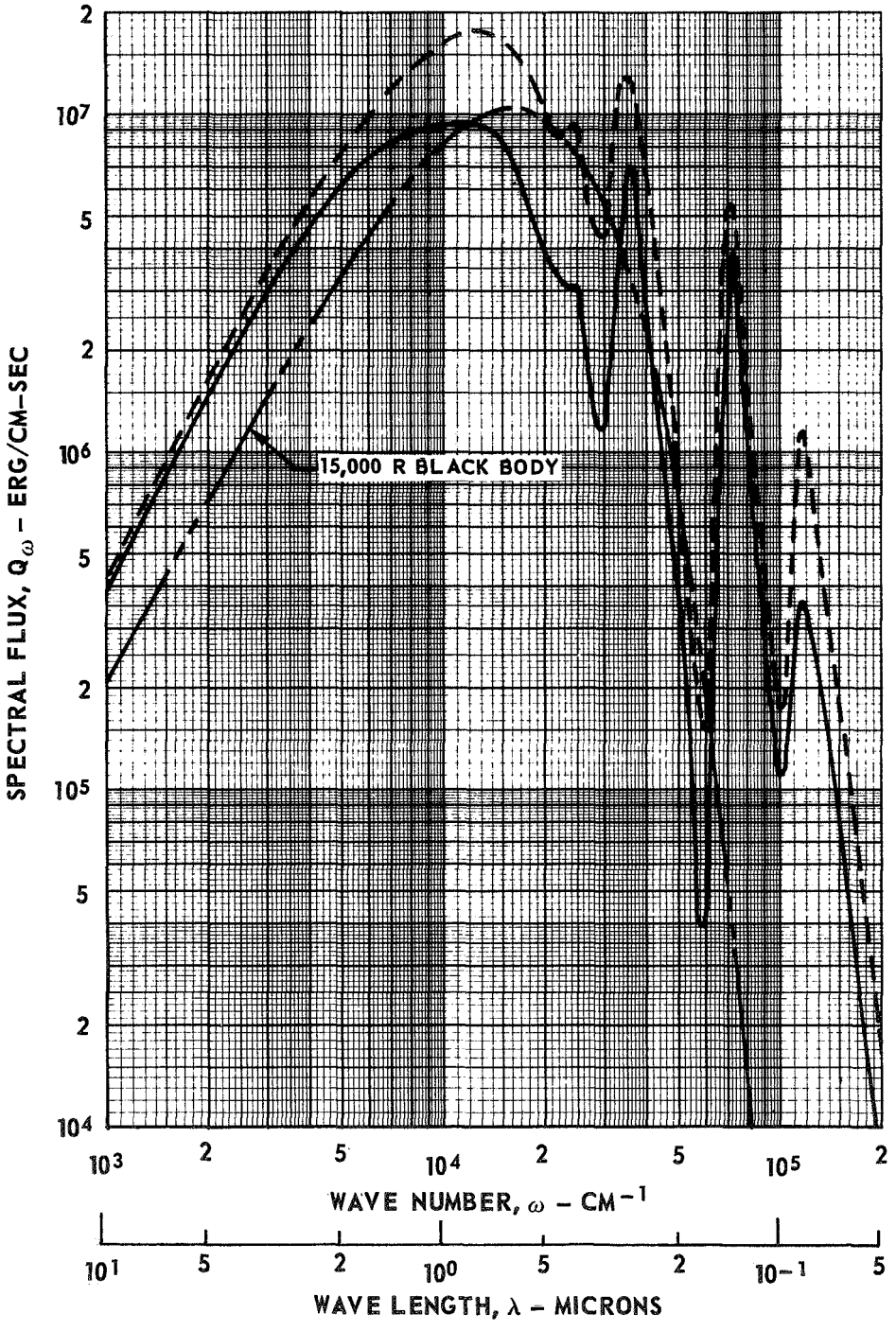

FIG. 19

COMPARISON OF FRACTIONAL FLUX DISTRIBUTION OF BLACK BODY AT TEMPERATURES OF 10,000, 15,000 AND 20,000 DEG R AND FRACTIONAL FLUX DISTRIBUTION EMITTED FROM NUCLEAR FUEL FOR CASES 1 AND 2

CASE & SYMBOL	T_E R	T* R	Q* BTU/FT^2 – SEC	SEED	r_ω
1 ———	10,650	15,000	24,300	—	0
2 — — — —	12,650	17,838	48,600	—	0

——— — — — BLACK BODY

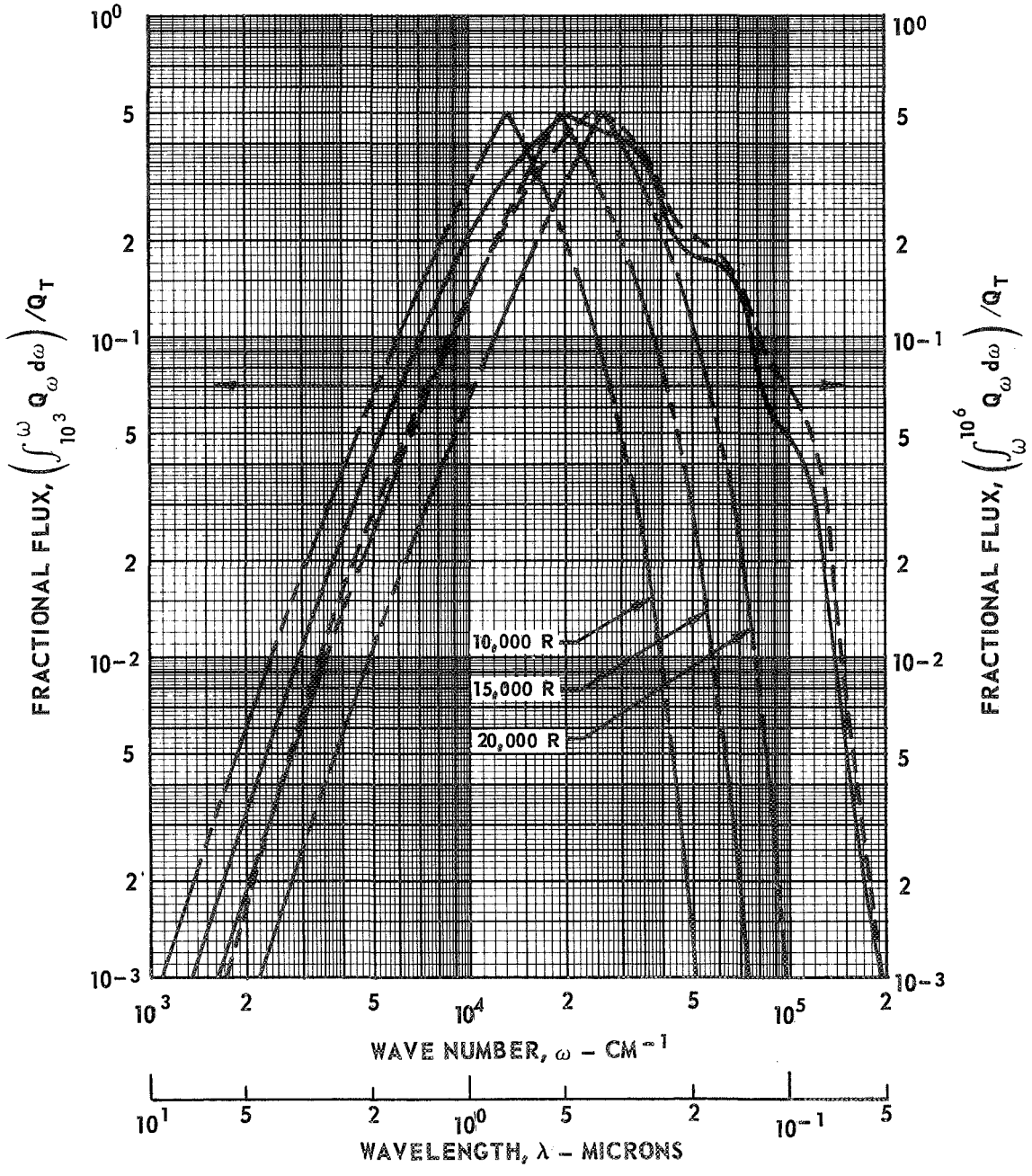

FIG. 20

COMPARISON OF SPECTRAL FLUX FOR A BLACK BODY AT A TEMPERATURE OF 15,000 DEG R AND SPECTRAL FLUX EMITTED FROM NUCLEAR FUEL FOR CASE 1 AND 3

CASE & SYMBOL	T_E R	T* R	Q* BTU/FT^2 – SEC	SEED	r_ω
1 ———	10,650	15,000	24,300	—	0
3 — — —	11,650	15,000	24,300	5 ATM– O_2 5 ATM – NO	0

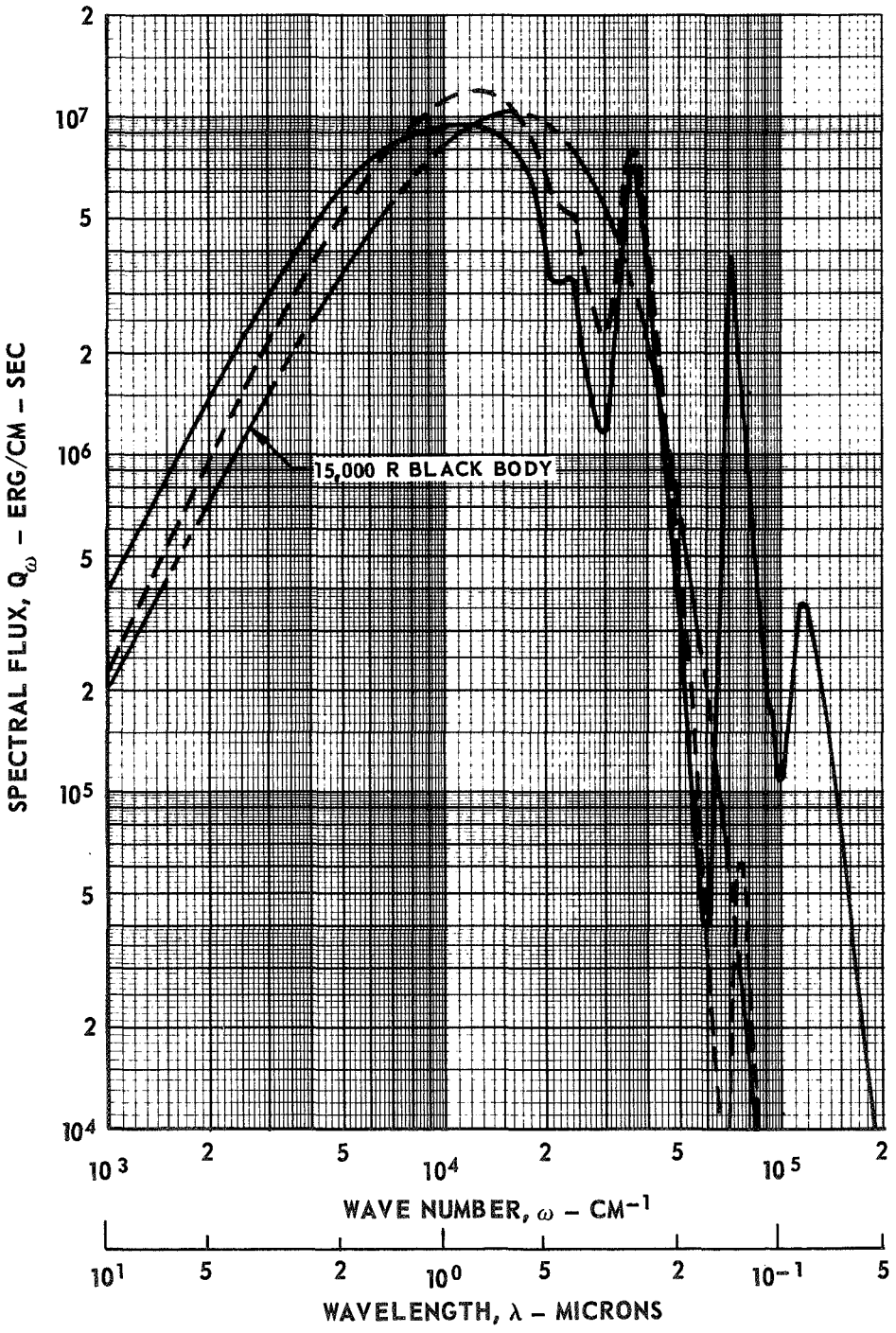

FIG. 21

COMPARISON OF FRACTIONAL FLUX DISTRIBUTION OF BLACK BODY AT TEMPERATURES OF 10,000, 15,000 AND 20,000 DEG R AND FRACTIONAL FLUX DISTRIBUTION EMITTED FROM NUCLEAR FUEL FOR CASES 1 AND 3

CASE & SYMBOL	T_E R	T* R	Q* BTU/FT^2 – SEC	SEED	r_ω
1 ———	10,650	15,000	24,300	—	0
3 — — —	11,650	15,000	24,300	5 ATM – O_2 5 ATM – NO	0

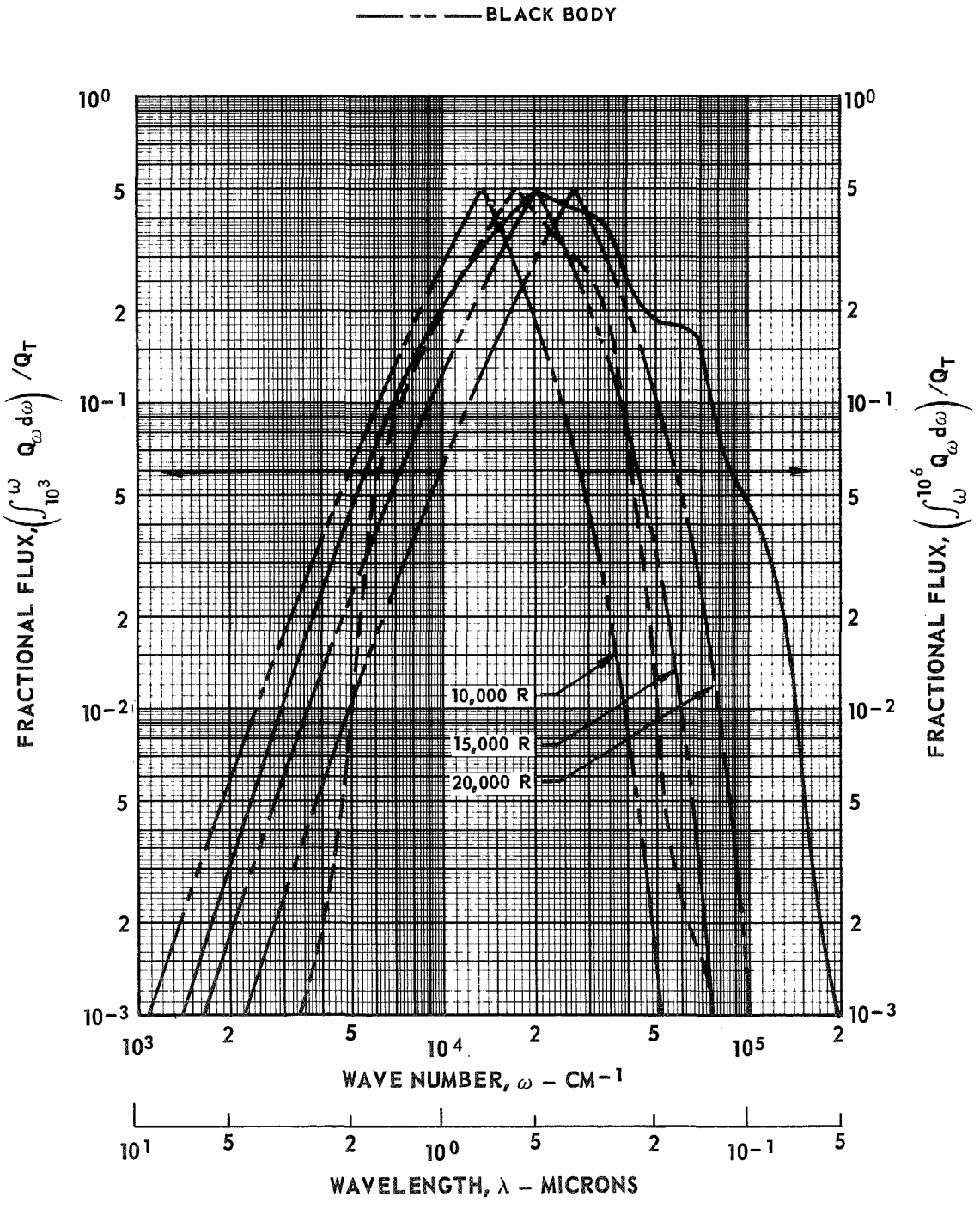

COMPARISON OF SPECTRAL FLUX FOR A BLACK BODY AT A TEMPERATURE OF 15,000 DEG R AND SPECTRAL FLUX EMITTED FROM NUCLEAR FUEL FOR CASES 1, 4 AND 5

CASE & SYMBOL	T_E R	T* R	Q* BTU/FT^2 – SEC	SEED	r_ω
1 ———	10,650	15,000	24,300	—	0
4 – – –	23,650	15,000	24,300	—	ALUMINUM
5 ——— – ———	17,650	15,000	24,300	—	SILVER

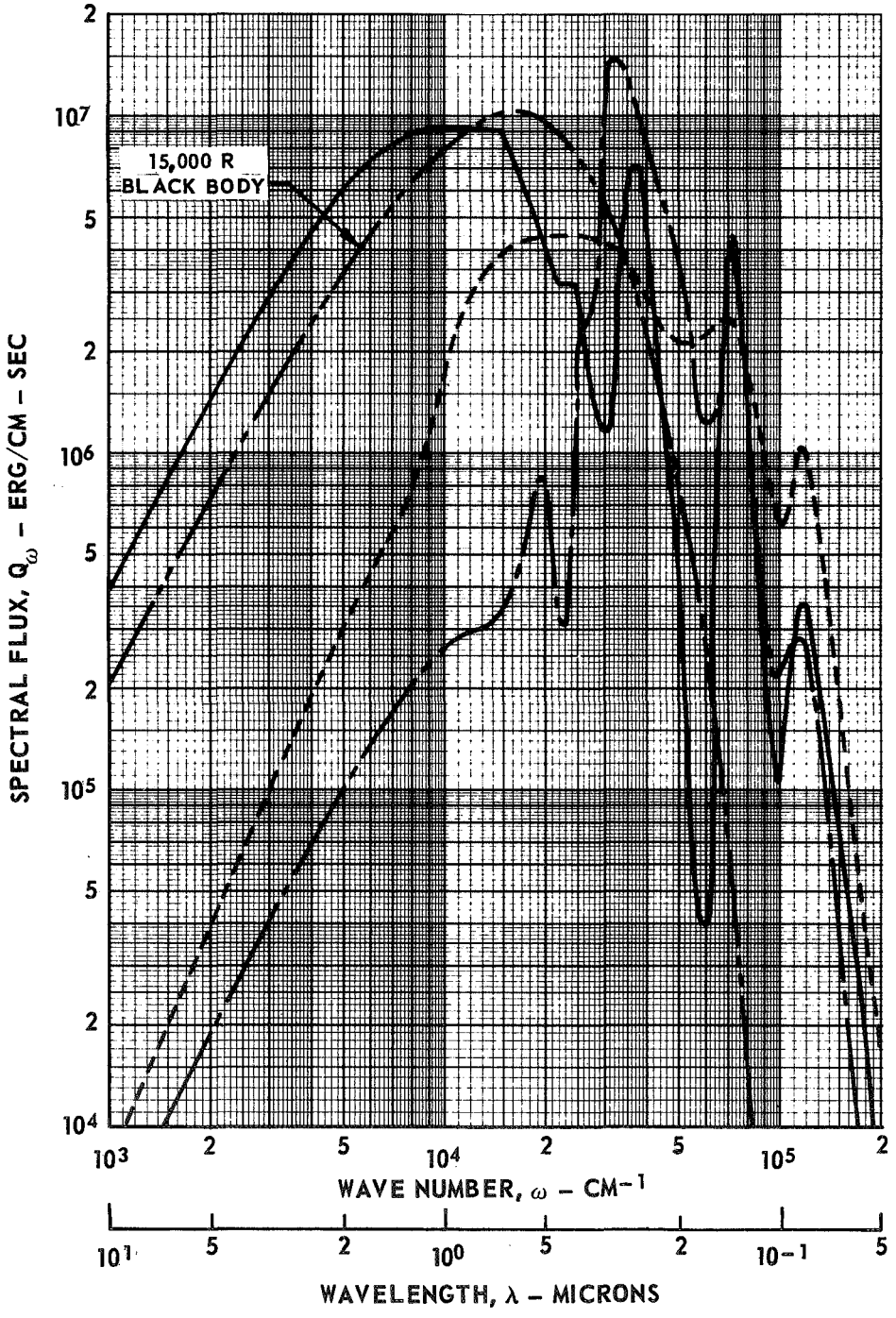

FIG. 23

COMPARISON OF FRACTIONAL FLUX DISTRIBUTION OF BLACK BODY AT TEMPERATURES OF 10,000 15,000 AND 20,000 DEG R AND FRACTIONAL FLUX DISTRIBUTION EMITTED FROM NUCLEAR FUEL FOR CASES 1, 4 AND 5

CASE & SYMBOL	T_E R	T* R	Q* BTU/FT^2 – SEC	SEED	r_ω
1 ———	10,650	15,000	24,300	—	0
4 — — —	23,650	15,000	24,300	—	ALUMINUM
5 ———	17,650	15,000	24,300	—	SILVER

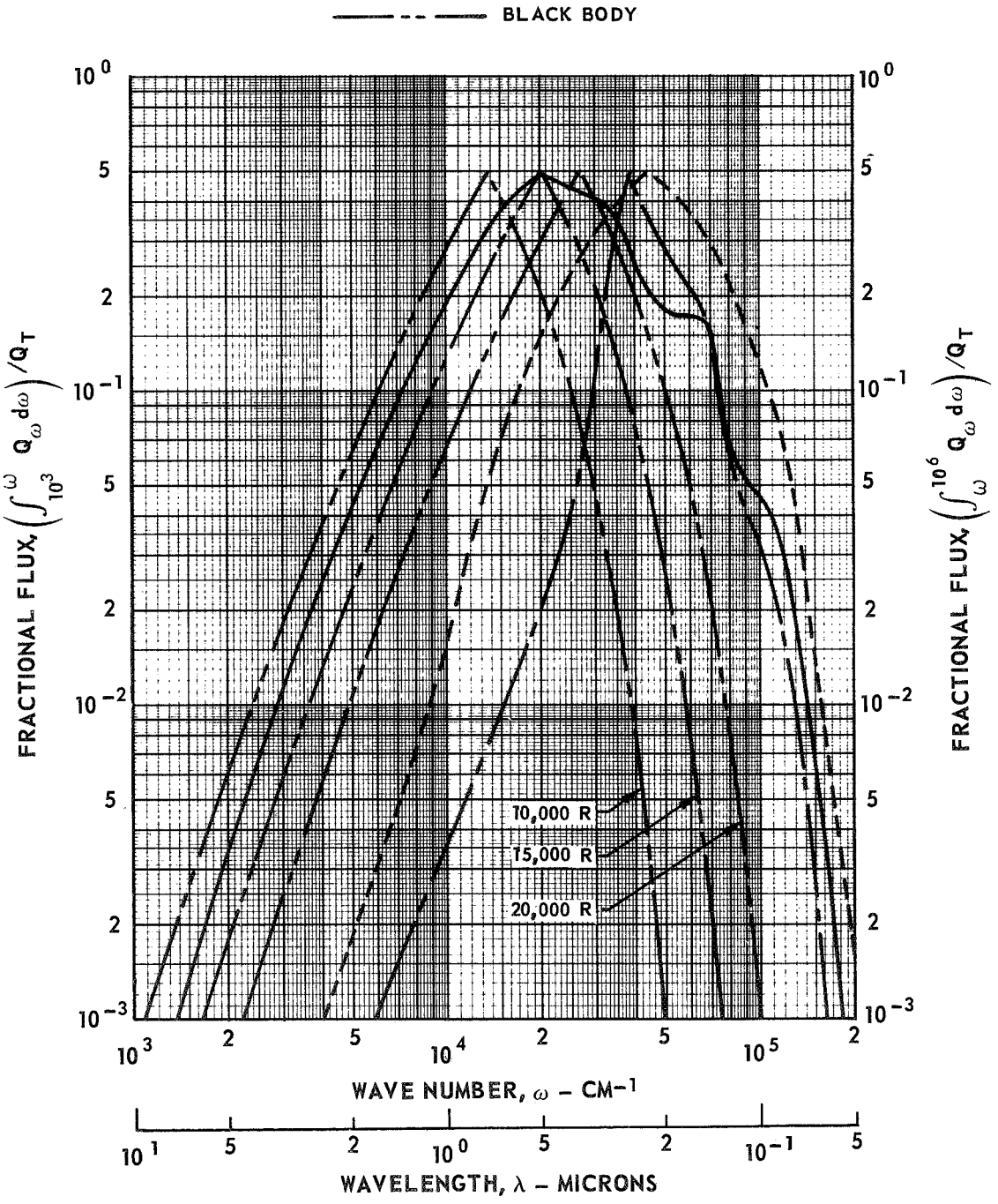

COMPARISON OF SPECTRAL FLUX FOR A BLACK BODY AT A TEMPERATURE OF 15,000 DEG R AND SPECTRAL FLUX EMITTED FROM NUCLEAR FUEL FOR CASES 1, 4 AND 6

CASE & SYMBOL	T_E R	T* R	Q* BTU/FT^2 – SEC	SEED	r_ω
1 ———	10,650	15,000	24,300	–	0
4 – – –	23,650	15,000	24,300	–	ALUMINUM
6 ———	24,650	15,000	24,300	5 ATM – O_2 5 ATM – NO	ALUMINUM

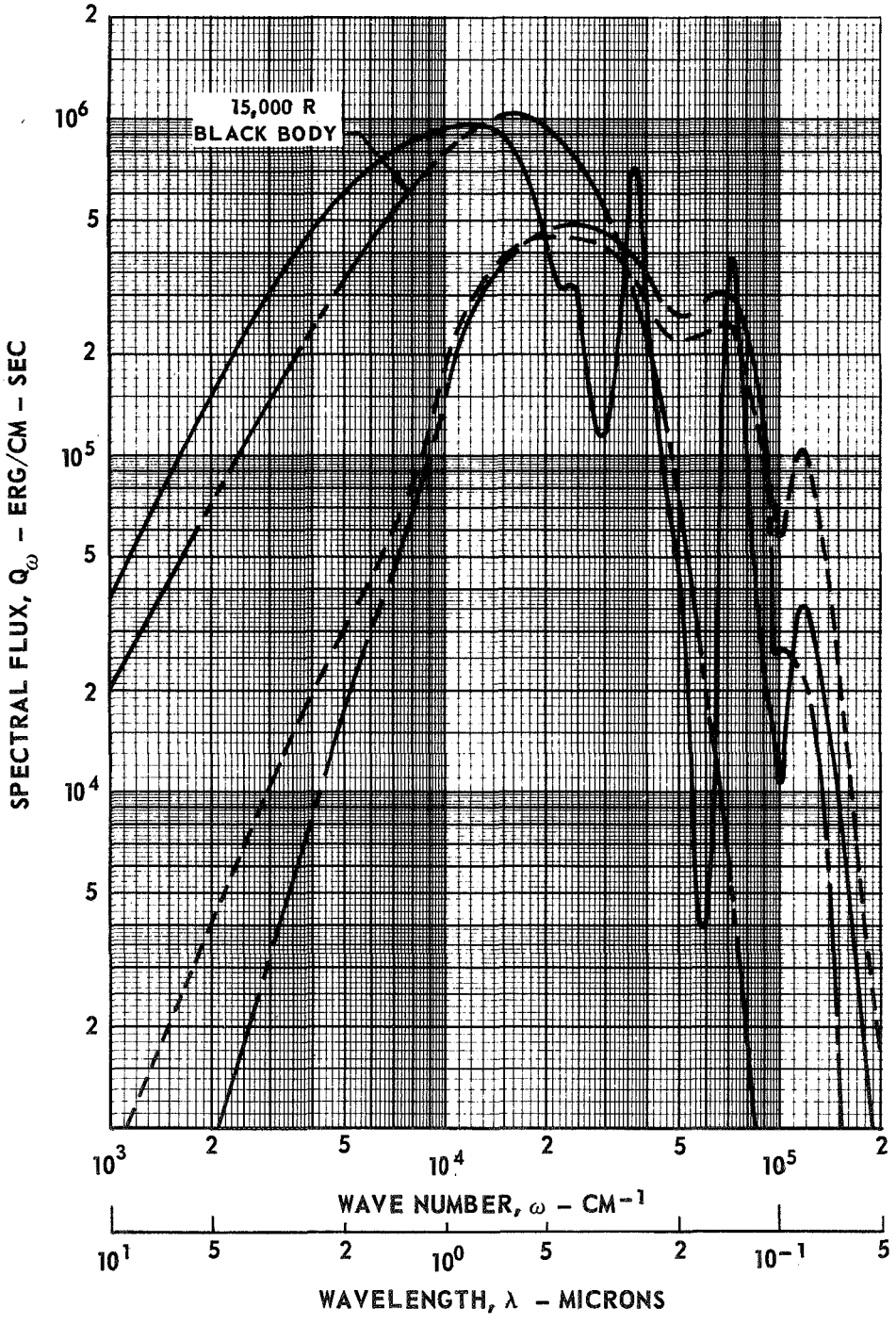

FIG. 25

COMPARISON OF FRACTIONAL FLUX DISTRIBUTION OF BLACK BODY AT TEMPERATURE OF 10,000, 15,000, 20,000 DEG R AND FRACTION FLUX DISTRIBUTION EMITTED FROM NUCLEAR FUEL FOR CASES 1, 4 AND 6

CASE & SYMBOL	T_E R	T* R	Q* BTU/FT^2 – SEC	SEED	r_ω
1 ———	10,650	15,000	24,300	–	0
4 — — —	23,650	15,000	24,300	–	ALUMINUM
6 — · —	24,650	15,000	24,300	5 ATM – O_2 5 ATM – NO	ALUMINUM

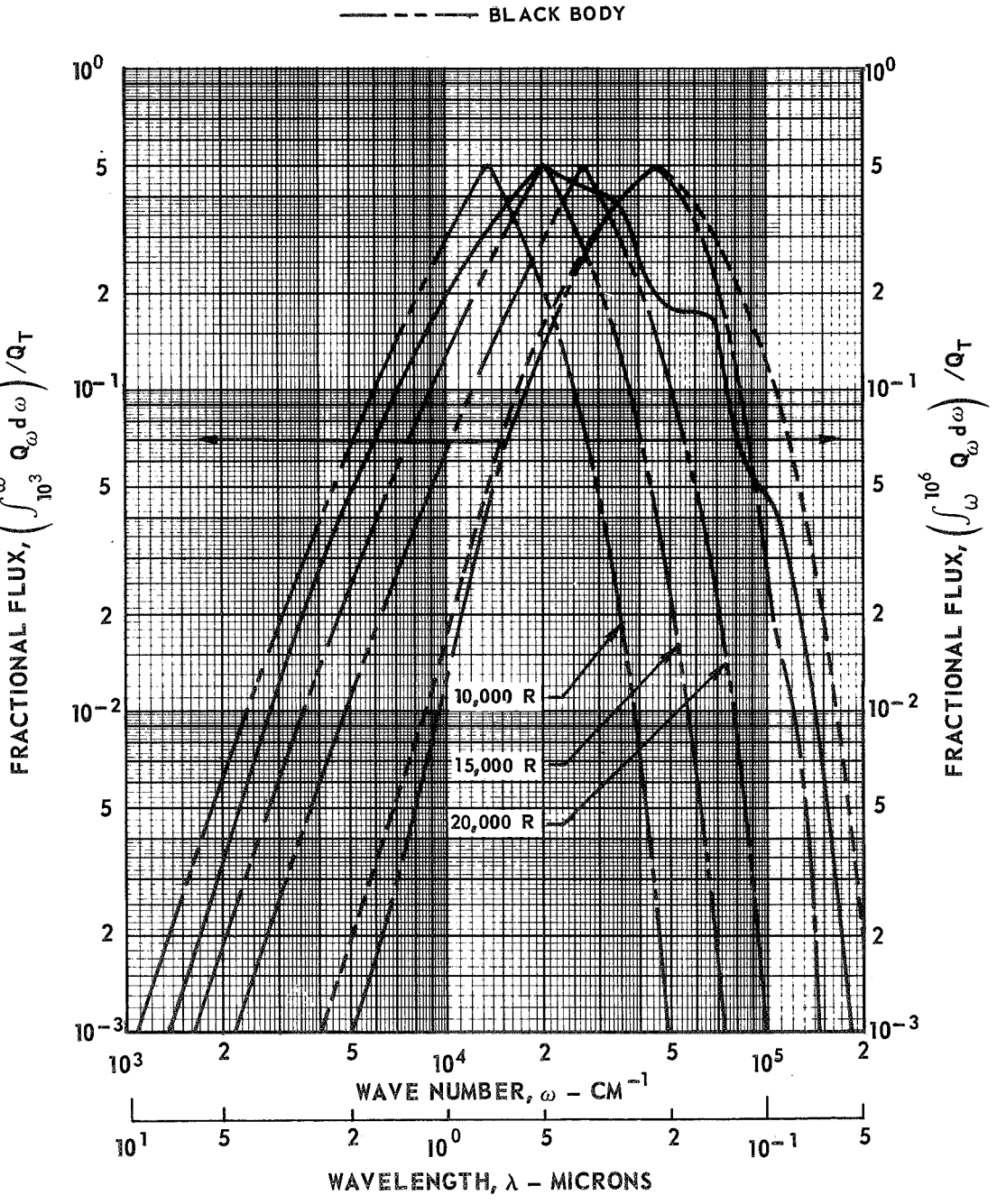

FIG. 26

OPTICAL DEPTH DISTRIBUTION AT REPRESENTATIVE WAVE NUMBERS FOR CASE 1

T_E = 10,650 R

T* = 15,000 R

Q* = 24,300 BTU/FT^2 - SEC

NO REFLECTIVE WALLS

NO SEED GASES

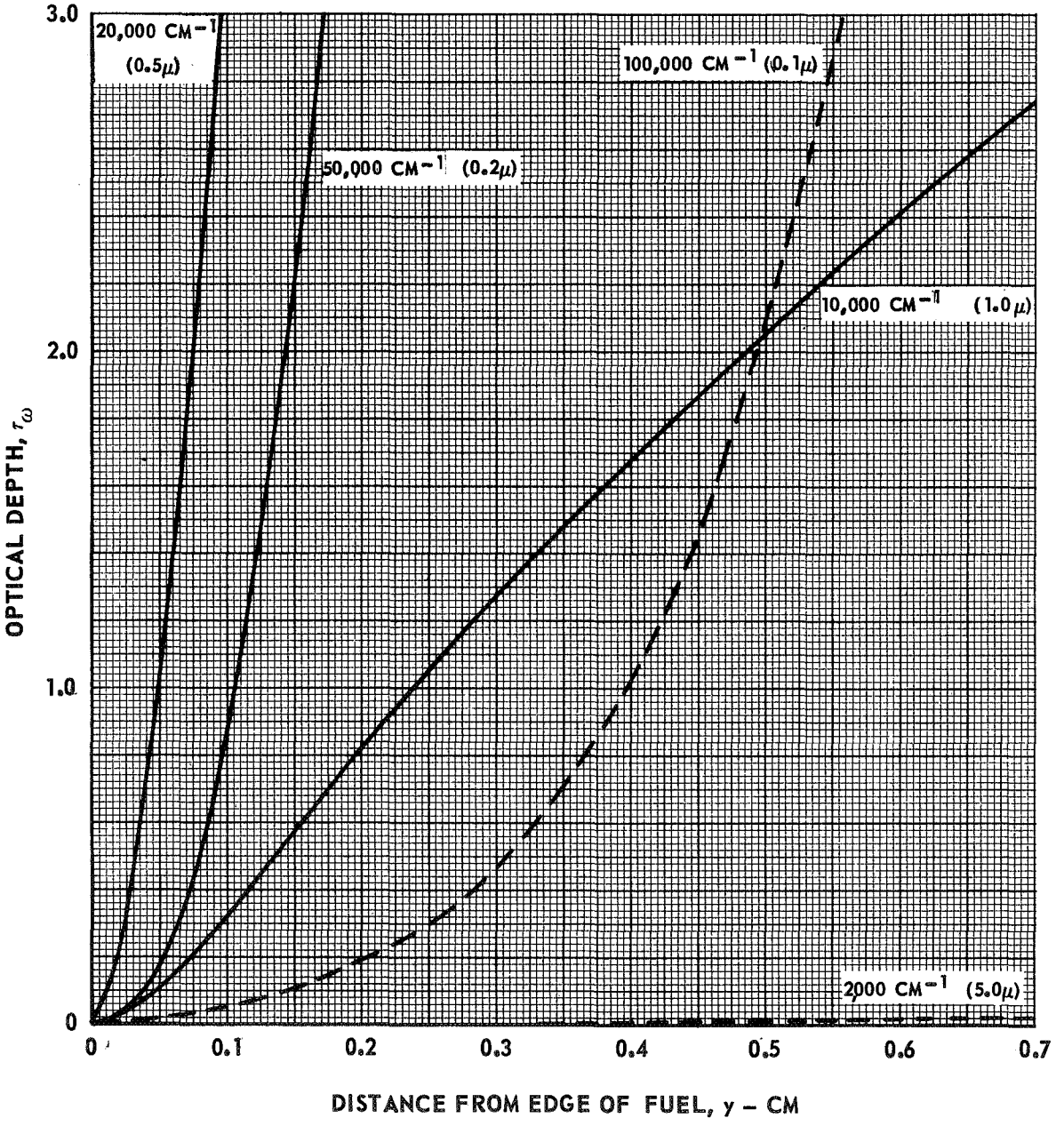

FIG. 27

OPTICAL DEPTH DISTRIBUTION AT REPRESENTATIVE WAVE NUMBERS FOR CASE 2

T_E = 12,650 R

T* = 17,838 R

Q* = 48,600 BTU/FT^2 - SEC

NO REFLECTIVE WALLS

NO SEED GASES

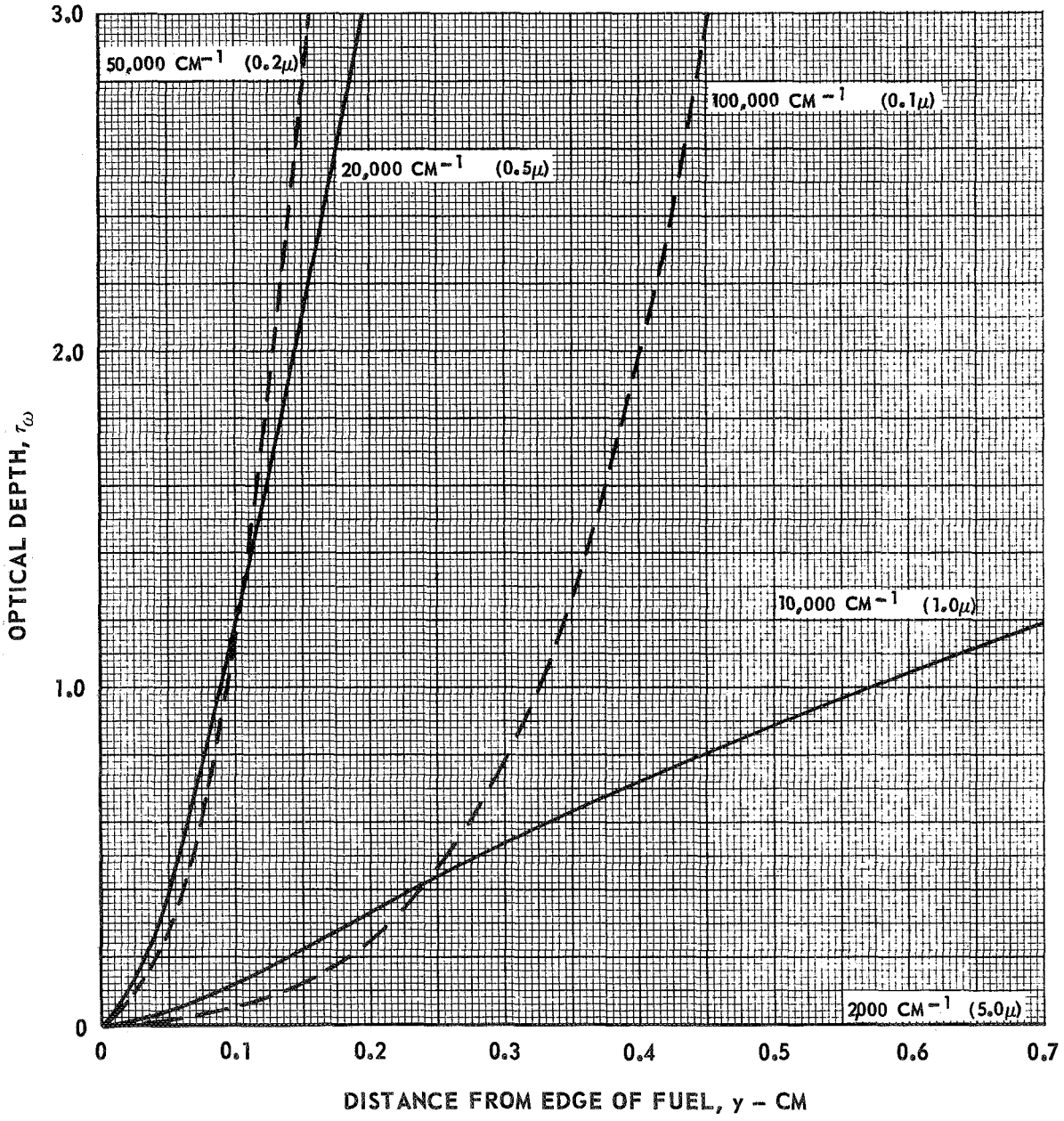

OPTICAL DEPTH DISTRIBUTION AT REPRESENTATIVE WAVE NUMBERS FOR CASE 3

T_E = 11,650 R

T* = 15,000 R

Q* = 24,300 BTU/FT^2 - SEC

NO REFLECTIVE WALLS

SEED - 5 ATM O_2 , 5 ATM NO

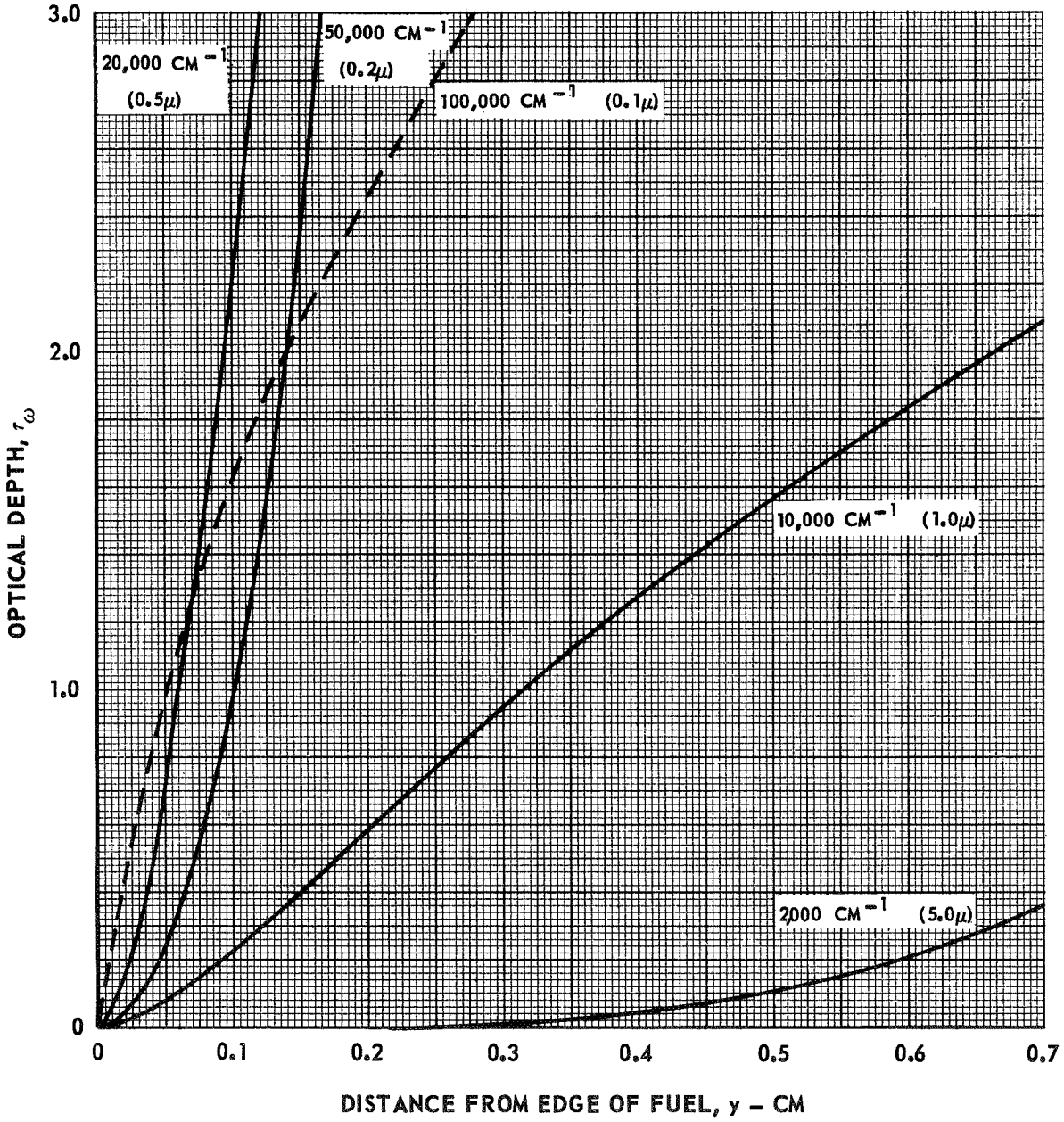

OPTICAL DEPTH DISTRIBUTION AT REPRESENTATIVE WAVE NUMBERS FOR CASE 4

T_E = 23,650 R

T* = 15,000 R

Q* = 24,300 BTU/FT^2 - SEC

REFLECTIVITY - ALUMINUM

NO SEED GASES

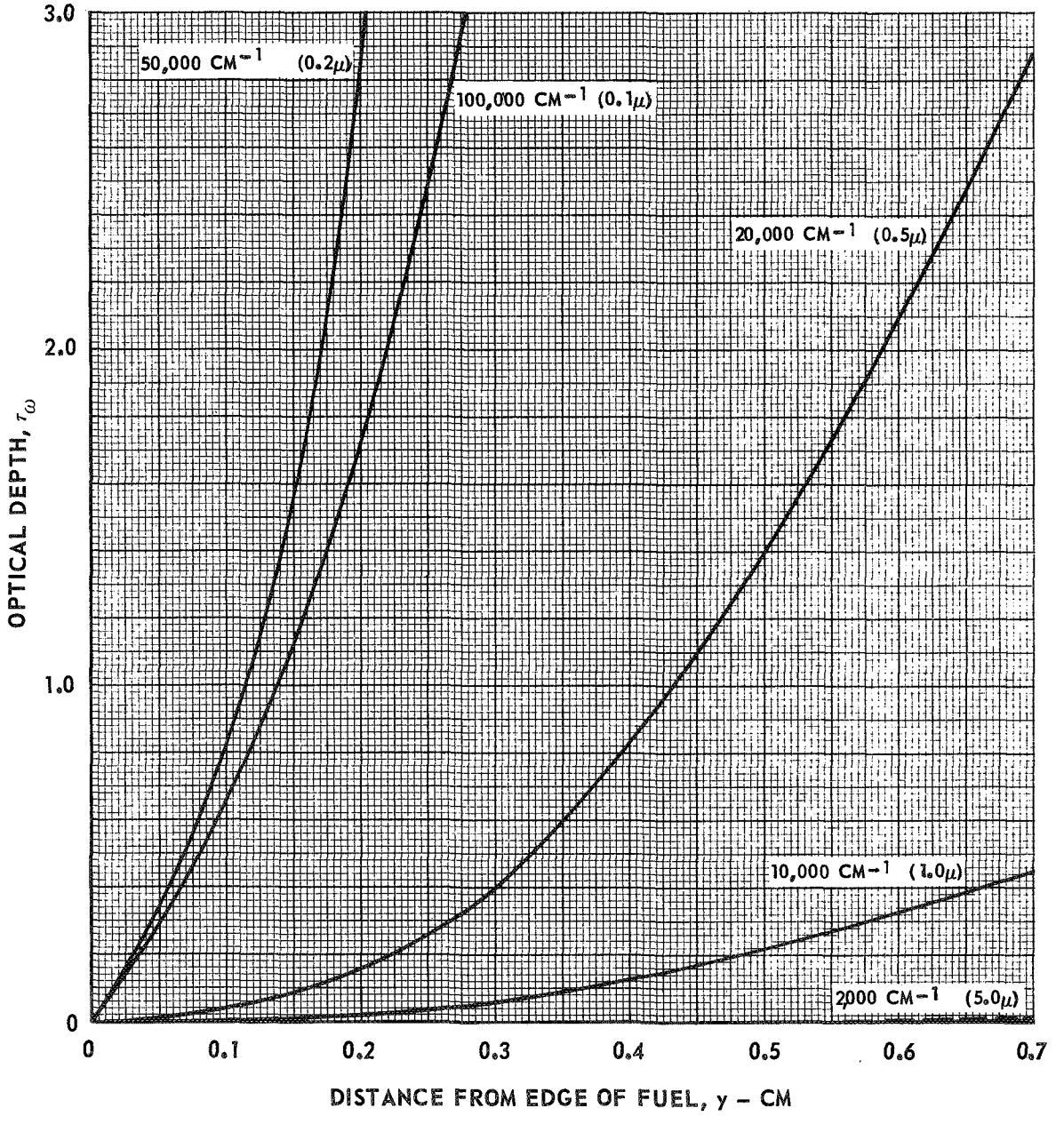

OPTICAL DEPTH DISTRIBUTION AT REPRESENTATIVE WAVE NUMBER FOR CASE 5

T_E = 17,650 R

T* = 15,000 R

Q* = 24,300 BTU/FT^2 – SEC

REFLECTIVITY – SILVER

NO SEED GASES

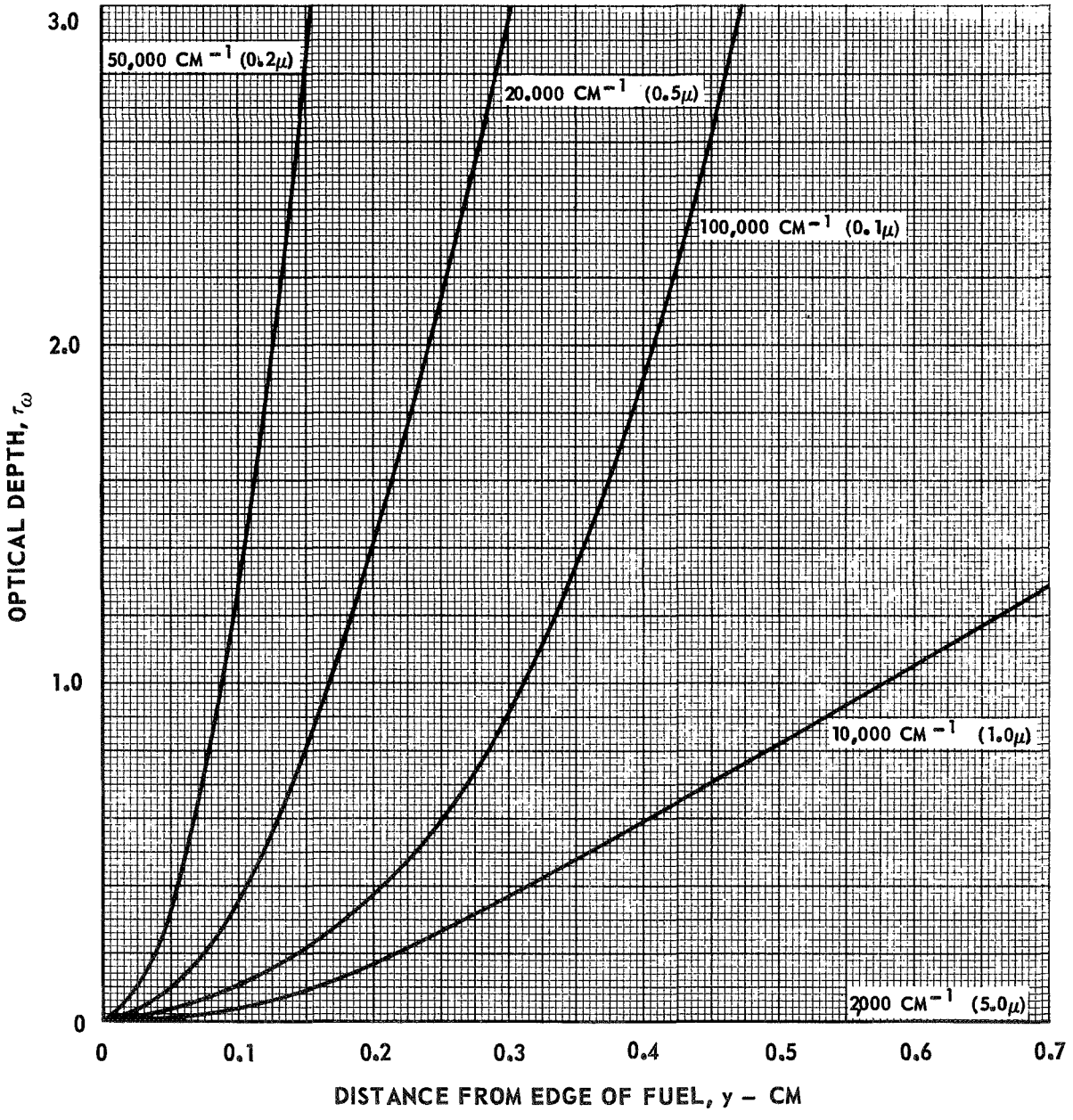

FIG. 31

OPTICAL DEPTH DISTRIBUTION AT REPRESENTATIVE WAVE NUMBERS FOR CASE 6

T_E = 24,650 R

T* = 15,000 R

Q* = 24,300 BTU/FT^2 – SEC

REFLECTIVITY – ALUMINUM

SEED – 5 ATM O_2, 5 ATM NO

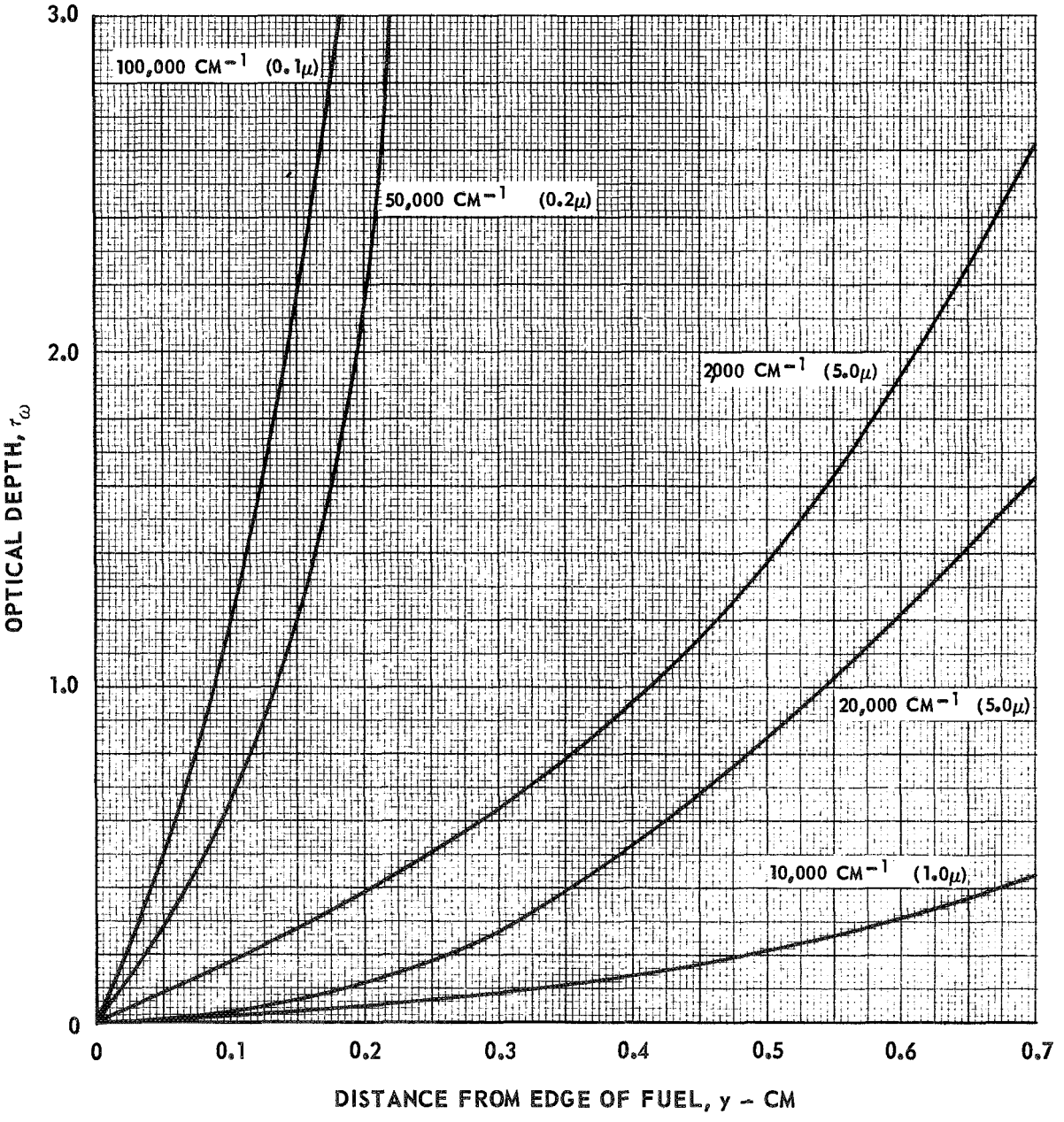

FIG. 32

BLACK - BODY SPECTRAL FLUX AS A FUNCTION OF TEMPERATURE AT REPRESENTATIVE WAVE NUMBERS

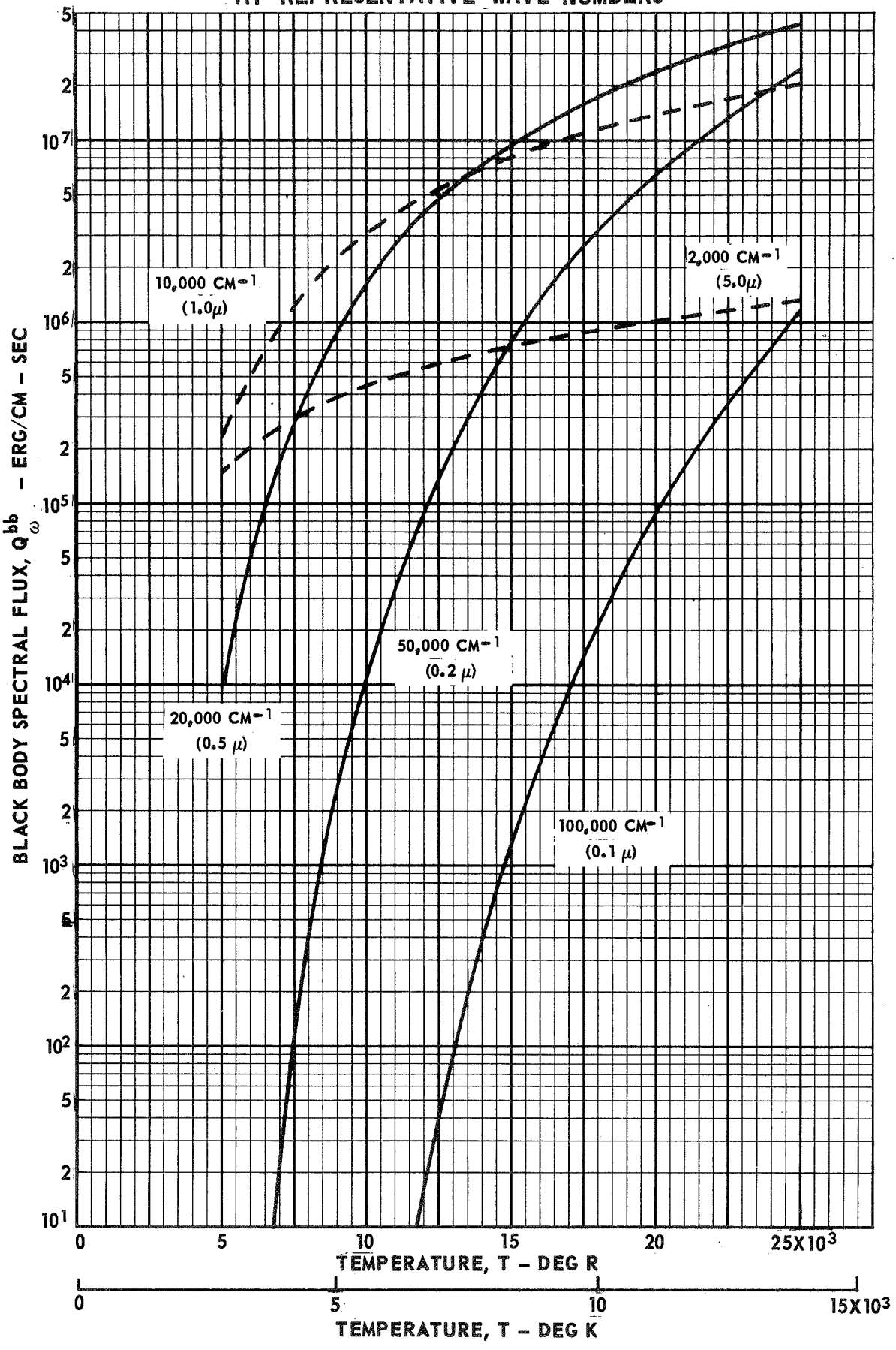

EFFECTIVE SPECTRAL BLACK BODY RADIATING TEMPERATURE AS A FUNCTION OF WAVE NUMBER FOR CASES 1 THROUGH 6

CASE	T_E R	T^* R	Q^* BTU/FT^2 – SEC	SEED	r_ω
1	10,650	15,000	24,300	—	0
2	12,650	17,838	48,600	—	0
3	11,650	15,000	24,300	5 ATM – O_2 5 ATM – NO	0
4	23,650	15,000	24,300	—	ALUMINUM
5	17,650	15,000	24,300	—	SILVER
6	24,650	15,000	24,300	5 ATM – O_2 5 ATM – NO	ALUMINUM

T_{bb} (ω) DEFINED AS THAT TEMPERATURE FOR WHICH $Q_\omega^{bb} = Q_\omega^{CASE\ i}$

(CASES INDICATED BY CIRCLED NUMERALS)

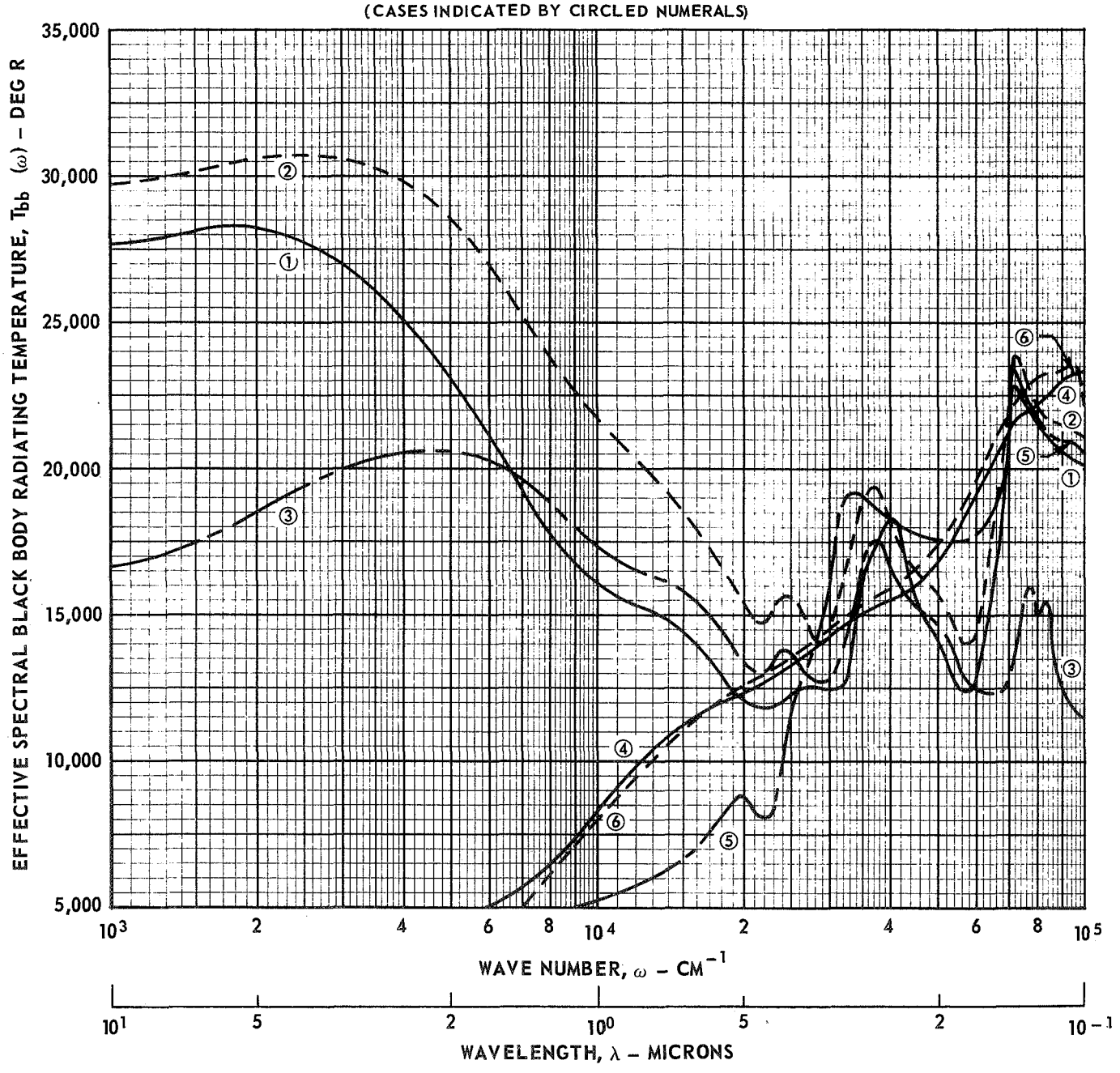

EFFECTIVE OPTICAL DEPTH AS A FUNCTION OF WAVE NUMBER FOR CASES 1 THROUGH 6

CASE	T_E R	T* R	Q* BTU/FT^2 – SEC	SEED	r_ω
1	10,650	15,000	24,300	–	0
2	12,650	17,838	48,600	–	0
3	11,650	15,000	24,300	5 ATM – O_2 5 ATM – NO	0
4	23,650	15,000	24,300	–	ALUMINUM
5	17,650	15,000	24,300	–	SILVER
6	24,650	15,000	24,300	5 ATM – O_2 5 ATM – NO	ALUMINUM

$\tau_{\omega,E}$ DEFINED AS THE OPTICAL DEPTH AT WHICH $T_{bb}(\omega)$ EQUALS GAS TEMPERATURE

(CASES INDICATED BY CIRCLED NUMBERS. SEE TEXT FOR CASES 4 & 6)

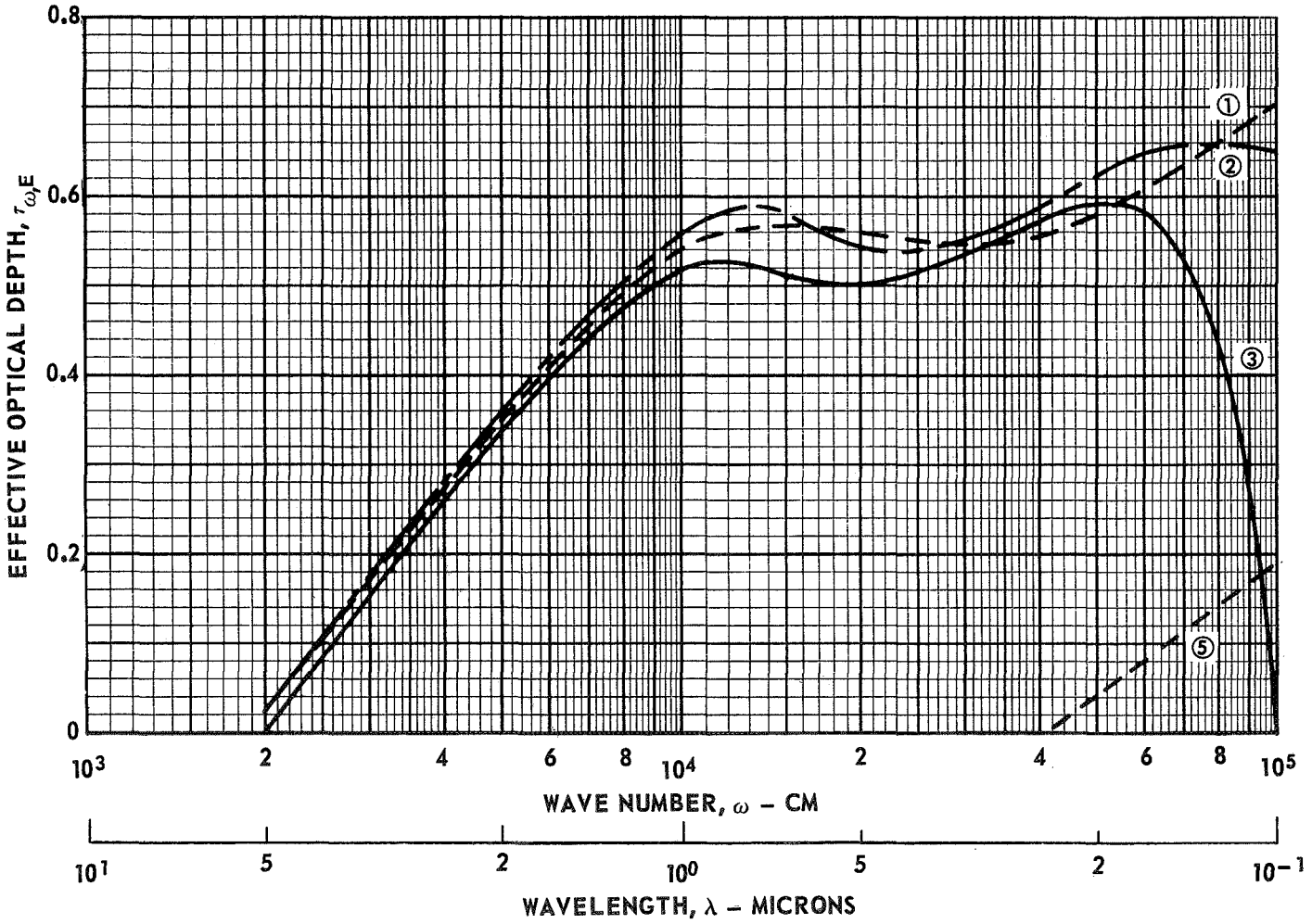


UNITED AIRCRAFT CORPORATION